blood

American Society of Hematology
2021 L Street NW, Suite 900,
Washington, DC 20036
Phone: 202-776-0544 | Fax 202-776-0545
editorial@hematology.org

A lineage-specific STAT5BN642H mouse model to study NK-cell leukemia

Tracking no: BLD-2023-022655R1

Klara Klein (University of Veterinary Medicine, Austria) Sebastian Kollmann (University of Veterinary Medicine, Austria) Angela Hiesinger (University of Veterinary Medicine Vienna, Institute of Pharmacology and Toxicology, Austria) Julia List (University of Veterinary Medicine Vienna, Institute of Pharmacology and Toxicology, Austria) Jonatan Kendler (University of Veterinary Medicine Vienna, Institute of Pharmacology and Toxicology, Austria) Thorsten Klampfl (University of Veterinary Medicine Vienna, Austria) Mehak Randhawa (University of Veterinary Medicine Vienna, Institute of Pharmacology and Toxicology, Austria) Jana Trifinopoulos (University of Veterinary Medicine Vienna, Institute of Pharmacology and Toxicology, Austria) Barbara Maurer (University of Veterinary Medicine Vienna, Institute of Pharmacology and Toxicology, Austria) Reinhard Grausenburger (University of Veterinary Medicine Vienna, Austria) Christof Bertram (University of Veterinary Medicine, Austria) Richard Moriggl (University of Veterinary Medicine, Austria) Thomas Rülicke (University of Veterinary Medicine, Vienna, Austria) Charles Mullighan (St Jude Children's Research Hospital, United States) Agnieszka Witalisz-Siepracka (University of Veterinary Medicine Vienna, Austria) Wencke Walter (Munich Leukemia Laboratory, Germany) Gregor Hoermann (MLL Munich Leukemia Laboratory, Germany) Veronika Sexl (University of Veterinary Medicine Vienna, Austria) Dagmar Gotthardt (University of Veterinary Medicine Vienna, Institute of Pharmacology and Toxicology, Austria)

Abstract:
Patients with T- and NK-cell neoplasms frequently have somatic STAT5B gain-of-function mutations. The most frequent STAT5B mutation is STAT5BN642H, which is known to drive murine T-cell leukemia although its role in NK-cell malignancies is unclear. Introduction of the STAT5BN642H mutation into human NK-cell lines enhances their potential to induce leukemia in mice. We have generated a mouse model that enables tissue-specific expression of STAT5BN642H and have selectively expressed the mutated STAT5B in hematopoietic cells (N642Hvav/+) or exclusively in NK cells (N642HNK/NK). All N642Hvav/+ mice rapidly develop an aggressive T-/NK T-cell leukemia, whereas N642HNK/NK mice display an indolent NK-large granular lymphocytic leukemia (NK-LGLL) that progresses to an aggressive leukemia with age. Samples from NK-cell leukemia patients have a distinctive transcriptional signature driven by mutant STAT5B, which overlaps with that of murine leukemic N642HNK/NK NK cells. We have generated the first reliable STAT5BN642H-driven pre-clinical mouse model that displays an indolent NK-LGLL progressing to aggressive NK-cell leukemia. This novel in vivo tool will enable us to explore the transition from an indolent to an aggressive disease and will thus permit the study of prevention and treatment options for NK-cell malignancies. -

Conflict of interest: COI declared - see note

COI notes: G.H and W.W: Employment by MLL Munich Leukemia Laboratory; C.G.M. received research funding from Pfizer and AbbVie, is on the Illumina Advisory Board and holds royalties in Cyrus and stocks in Amgen.

Preprint server: Yes; bioRxiv https://doi.org/10.1101/2023.10.04.560502

Author contributions and disclosures: K.K., V.S. and D.G. conceived the study; T. R. and K.K. generated the mouse model. K.K., S.K., A.H., M.R, J.L., J.T., J.K. and D.G. performed the experiments. K.K., S.K. and D.G. analyzed the data. A.W.S., C.A.B. and B.M. established methods and helped with the experiments and analysis of the data. R.M. and C.G.M. were involved in experimental design and scientific discussions; R.G., T.K., J.K. and S.K analyzed sequencing data; G.H., W.W. and C.G.M. provided bioinformatic patient data analysis; D.G., K.K., S.K., and V.S. wrote the manuscript. D.G. and V.S. provided reagents and supervised the study. All authors revised the manuscript.

Non-author contributions and disclosures: Yes; Graham Tebb, University of Veterinary Medicine Vienna: proofread the manuscript.

Agreement to Share Publication-Related Data and Data Sharing Statement: The RNA-Seq data reported in this article have been deposited in the ArrayExpress database (Accession ID: E-MTAB-13797).

Clinical trial registration information (if any):

A lineage-specific *STAT5B*^{N642H} mouse model to study NK-cell leukemia

Running title: Mutant STAT5B triggers NK-cell neoplasms

Klara Klein[1#], Sebastian Kollmann[1#], Angela Hiesinger[1], Julia List[1], Jonatan Kendler[1], Thorsten Klampfl[1], Mehak Rhandawa[1], Jana Trifinopoulos[1], Barbara Maurer[1], Reinhard Grausenburger[1], Christof A. Betram[2], Richard Moriggl[3], Thomas Rülicke[4], Charles G. Mullighan[5], Agnieszka Witalisz-Siepracka[1,6], Wencke Walter[7], Gregor Hoermann[7], Veronika Sexl[1,8*], & Dagmar Gotthardt[1*]

[1] Department of Biomedical Sciences, University of Veterinary Medicine, Vienna, Austria
[2]Institute of Pathology, University of Veterinary Medicine, Vienna, Austria
[3]Institute of Animal Breeding and Genetics, Unit for Functional Cancer Genomics, University of Veterinary Medicine, Vienna, Austria
[4]Department of Biomedical Sciences and Ludwig Boltzmann Institute for Hematology and Oncology, University of Veterinary Medicine Vienna, Vienna, Austria
[5]Department of Pathology and the Hematological Malignancies Program, St. Jude Children's Research Hospital, Memphis, TN, USA
[6]Department of Pharmacology, Physiology and Microbiology, Division Pharmacology, Karl Landsteiner University of Health Sciences, Krems, Austria
[7]MLL Munich Leukemia Laboratory, Munich, Germany
[8]University of Innsbruck, Innsbruck, Austria

# equally contributed

* equally contributed

Corresponding author:
Dagmar Gotthardt, PhD
Institute of Pharmacology and Toxicology
University of Veterinary Medicine Vienna
Veterinaerplatz 1, A-1210 Vienna. Austria
Phone: +431 25077 2900
Email: dagmar.gotthardt@vetmeduni.ac.at

Data Sharing Statement

All other relevant data that support the conclusions of the study are available from the authors on request. Please contact dagmar.gotthardt@vetmeduni.ac.at. The RNA-Seq data reported in this article have been deposited in the ArrayExpress database (Accession ID: E-MTAB-13797).

Text word count: 3887

Abstract word count: 187
Main Figures: 7
Suppl. Figures: 7
Suppl. Tables: 5
Main References: 100
Suppl. References: 16
Key words: STAT5B^{N642H}, STAT5B-driven mouse model, NK-cell leukemia
Key points:

- Generation of a lineage-specific *STAT5B*^{N642H} transgenic mouse model which develops NK-cell leukemia
- Leukemic NK cells with a *STAT5B* gain of function mutation share a unique transcriptional profile in mice and human patients

Abstract

Patients with T- and NK-cell neoplasms frequently have somatic *STAT5B* gain-of-function mutations. The most frequent *STAT5B* mutation is *STAT5B*^{N642H}, which is known to drive murine T-cell leukemia although its role in NK-cell malignancies is unclear.

Introduction of the *STAT5B*^{N642H} mutation into human NK-cell lines enhances their potential to induce leukemia in mice. We have generated a mouse model that enables tissue-specific expression of *STAT5B*^{N642H} and have selectively expressed the mutated *STAT5B* in hematopoietic cells (N642H$^{vav/+}$) or exclusively in NK cells (N642H$^{NK/NK}$). All N642H$^{vav/+}$ mice rapidly develop an aggressive T-/NK T-cell leukemia, whereas N642H$^{NK/NK}$ mice display an indolent NK-large granular lymphocytic leukemia (NK-LGLL) that progresses to an aggressive leukemia with age. Samples from NK-cell leukemia patients have a distinctive transcriptional signature driven by mutant STAT5B, which overlaps with that of murine leukemic N642H$^{NK/NK}$ NK cells.

We have generated the first reliable *STAT5B*^{N642H}-driven pre-clinical mouse model that displays an indolent NK-LGLL progressing to aggressive NK-cell leukemia. This novel *in vivo* tool will enable us to explore the transition from an indolent to an aggressive disease and will thus permit the study of prevention and treatment options for NK-cell malignancies.

Introduction

Natural Killer (NK)-cell malignancies are rare types of cancer that originate from the abnormal growth and proliferation of NK cells. They can be aggressive and challenging to treat. The World Health Organization distinguishes the following types of NK-cell neoplasms: extranodal NK/ T-cell lymphoma (ENKL), aggressive NK-cell leukemia (ANKL), chronic active Epstein-Barr virus (EBV) infection of NK cells (CAEBV) and NK-large granular lymphocytic leukemia (NK-LGLL), formerly called chronic lymphoproliferative disorder of NK cells (CLPD-NK)[1]. ENKL and ANKL are EBV-positive and associated with a poor prognosis[1]. NK-LGLL is usually EBV-negative, represents a subset of LGLL and is largely an indolent disease that may develop into an aggressive NK-cell malignancy[1–6]. The factors that trigger the transformation of an indolent into an aggressive form of NK-cell leukemia are unknown.

Signal transducer and activator of transcription 5 (STAT5) is a crucial component of the Janus kinase (JAK)/STAT pathway essential for the survival, proliferation and functionality of various hematopoietic cell types[7]. In leukemia, STAT activity is often enhanced by aberrant upstream tyrosine kinase activation, copy number gains[8] or activating mutations within STAT3/5B proteins themselves[9–14]. STAT5 is the most frequently deregulated member of the JAK/STAT family in hematopoietic cancer[15–17]. It comprises two individual genes, *STAT5A* and *STAT5B*, which express proteins with high homology[7,18–20]. Although STAT5A and STAT5B have largely redundant functions, they both have some individual roles[18,21]. STAT5B is the dominant gene product in T and NK cells and promotes their survival, proliferation, and cytotoxicity. *Stat5b*-deficient mice show reduced NK cell numbers and humans with a STAT5B deficiency suffer from immunodeficiencies caused by impairment in T-, regulatory T- (T_{reg}), and NK-cell differentiation and activation[18,22,31,32,23–30].

Activating *STAT5* mutations in hematological cancer predominantly occur in *STAT5B*[18]. The most frequent *STAT5B* gain-of-function (GOF) mutation, *STAT5B*^{N642H}, has been described in various forms of lymphoproliferative disorders, including T-cell lymphoma/leukemia, γδ-T-cell lymphoma, LGLL and NK-cell malignancies[9,11,39–43,13,14,33–38]. Activating *STAT5B* mutations have been detected in various NK-cell malignancies including cases of NK-LGLL and are linked to an aggressive clinical course[5,6,11,14,40,41,43–46]. *STAT5B*^{N642H} gives a proliferative advantage to human NK cells[43], but whether it alone is sufficient to drive NK-cell leukemia remains unknown.

Compared to the wild type allele, *STAT5B*^{N642H} enhances dimer stability and causes elevated and prolonged STAT5B tyrosine phosphorylation. As a consequence, STAT5B target gene expression is increased[9–11,34,39,42]. But even in the presence of activating *STAT5B* mutations, upstream cytokine signaling is necessary to activate JAK/STAT5 signaling[10,43,47]. In immune cells, STAT5 signaling is induced by various cytokines, including interleukin (IL)-2, IL-7 and IL-15, which promote cell proliferation, survival and maturation[48,49]. IL-15 overexpression has been implicated in leukemogenesis as IL-15 transgenic mice develop NK- or NKT-cell leukemia[50–52]. Another transgenic mouse model expressing human IL-15 and a transgenic mouse model expressing human *STAT5B*^{N642H} in the hematopoietic system under the *vav* promoter (vav-N642H) develop a lethal CD8$^+$ T-cell expansion[10,53]. The rapid development of the highly aggressive CD8$^+$ T-cell disease may mask and prevent the development of other malignancies as transplantation of NKT or γδ T cells from vav-N642H mice lead to leukemia developmen[9,54]. To investigate the oncogenic potential of *STAT5B*^{N642H} in other cell types, we generated a lox-stop-lox *STAT5B*^{N642H} transgenic mouse model that enables lineage-restricted transgene expression driven by cell type-specific expression of the *Cre* recombinase. The use of *Cre* recombinase under an NKp46$^+$ cell-specific promoter allows us to study the role of *STAT5B*^{N642H} in NK cells (N642H$^{NK/NK}$ mice). Here, the transcriptional changes associated with *STAT5B*^{N642H} expression in leukemic NK cells closely resemble disease signatures of human NK-cell leukemia with *STAT5B* GOF mutations, enabling the assessment of further treatment options utilizing the novel NK-cell leukemia model.

Materials and Methods

Conditional N642H mouse generation

Rosa26 (R26)-targeted lox-stop-lox STAT5B and STAT5B^{N642H} knock-in mice were generated using a STOP-EGFP-ROSA-CAG (SERCA) targeting vector[55] (obtained from Prof. Wunderlich, University Koeln). This vector integrates into the R26 locus enabling transgene expression under the CAG promoter coupled to IRES-controlled eGFP expression upon Cre recombinase-mediated excision of the floxed STOP-cassette. C-terminally V5-tagged human *STAT5B* or *STAT5B*^{N642H} transgenes were cloned downstream of the STOP cassette into the SERCA targeting vector. A control construct lacking a transgene but containing IRES-controlled eGFP downstream of the STOP cassette was included. The three R26-LSL knock-in lines B6-*Gt(ROSA)26Sor*$^{tm1(STAT5B-N642H)}$Biat, B6-*Gt(ROSA)26Sor*$^{tm2(STAT5B)}$Biat and B6-*Gt(ROSA)26Sor*$^{tm3(EGFP)}$Biat were generated using the linearized vectors for electroporation into C57BL/6N embryonic stem (ES) cells (parental ES cell line C2, Stock Number: 011989-

MU, Citation ID: RRID: MMRRC_011989-MU). Positively screened ES cell clones were injected into BALB/c blastocysts,transferred to pseudopregnant mice and chimeric offspring were bred with C57BL/6N mice.Germ-line transmission was confirmed by PCR (forward primers: *5′-GCACTTGCTCTCCCAAAGTCGCTC-3′* (R26_wt_fw) and *5′-CGCCGACCACTACCAGCAGAACAC-3′* (R26_EGFP_fw); reverse primer: *5′-ACAACGCCCACACACCAGGTTAGC-3′* (R26_wt_rev)) and selected for further crossing to Cre lines.

RNA-Seq of aged mouse NK cells

Frozen liver samples from aged non-diseased and diseased mice (healthy Cre neg (n=3), $GFP^{NK/NK}$ (n=2), $STAT5B^{NK/NK}$ (n=3) and $N642H^{NK/NK}$ (n=5), diseased $N642H^{NK/NK}$ (n=8)) were thawed and (GFP^{+}) $CD3^{-}NK1.1^{+}$ NK cells (and additionally $CD3^{+}NK1.1^{+}$ cells from #8) were sorted into a SMARTSeq lysis buffer using a CytoFlex SRT Sorter (Beckman Coulter). Libraries were constructed using the SMART-SEQ3 method[56] at the Vienna BioCenter Core facilities (VBCF), member of the Vienna Biocenter (VBC), Austria. Sequencing was performed on an Illumina NovaSeq 6000 system (Illumina, San Diego, CA, USA, 50-bp paired-end). Sequencing reads were quality controlled using the FastQC software (version 0.12.1)[57]. Detailed RNA-Seq analysis was performed as described in the Supplementary Methods. The RNA-Seq data reported in this article have been deposited in the ArrayExpress database (Accession ID: E-MTAB-13797).

Human patient data

Primary samples were obtained from bone marrow (BM) or peripheral blood of patients diagnosed with NK-cell neoplasms (n=64) or healthy donors (peripheral blood mononuclear cells (PBMCs)) after informed consent. Three patients harbored activating *STAT5B* mutations previously described[44] (one with $STAT5B^{N642H}$mutation, a second with $STAT5B^{Q706L}$ mutation and the third with both $STAT5B^{Y665F}$ and $STAT5B^{V712E}$ mutations). DNA and RNA were isolated from total leukocytes, followed by whole-genome- and RNA-sequencing at the Munich Leukemia Laboratory as previously described[58]. Reads were aligned to human reference genome (GRCh37, Ensembl annotation) using Isaac aligner (v3.16.02.19). Tumor-unmatched normal variant calling was performed with a pool of sex-matched DNA (Promega, Madison, WI) using Strelka (v.2.4.7). Variants were queried against the gnomAD database (v.2.1.1) to remove common germline calls and annotated with Ensembl VEP. Analysis was restricted to protein-altering and canonical splice-site variants. For transcriptome analysis, the TruSeq Total Stranded RNA kit was used, starting with 250ng of total RNA, to generate RNA

libraries following the manufacturer's recommendations (Illumina, San Diego, CA, USA). 2x100bp paired-end reads were sequenced on the NovaSeq 6000 (Illumina, San Diego, CA, USA) with a median of 50 million reads per sample. Reads were mapped with STAR aligner (v2.5.0a) to the human reference genome hg19 (RefSeq annotation). Gene- and transcript-specific read abundance was calculated with Cufflinks (v2.2.1). For gene expression analysis, estimated read counts for each gene were normalized by Trimmed mean of M-values (TMM) normalization and the resulting log2 counts per million (CPMs) were used.

Statistical analysis

The appropriate statistical method was used based on testing for normal distribution and homogeneity of variance. Tests were performed using GraphPad Prism. The statistical test is indicated in the corresponding figure legend.

Animal experiments were discussed and approved by the Ethics and Animal Welfare Committee of the University of Veterinary Medicine Vienna and the national authority (Austrian Federal Ministry of Education, Science and Research) in accordance with good scientific practice guidelines and national legislation, under licenses BMBWF-68.205/0103-WF/V/3b/2015, BMBWF-68.205/0010-V/3b/2019, BMBWF-68.205/0174-V/3b/20182022-0.762.012, 2023-0.108.862, 2022-0.404.452.

Results

N642H$^{vav/+}$ mice develop a hematopoietic malignancy

We generated mice with a human V5-tagged *STAT5B*^{N642H} transgene and IRES-eGFP under the CAG promoter downstream of a lox-stop-lox-cassette integrated into the *Rosa26* locus. The animals were crossed to *Vav*-Cre mice[59] (N642H$^{vav/+}$) to study the effects of *STAT5B*^{N642H} on the hematopoietic system (**Figure 1A**). We validated the presence of the STAT5B^{N642H} transgene by analyzing expression of eGFP and the V5 tag in N642H$^{vav/+}$ mice (**Figure 1B, S1A+B**). N642H$^{vav/+}$ BM cells displayed increased levels of tyrosine-phosphorylated STAT5 (pYSTAT5) compared to control BM cells, although reduced levels when compared to the pYSTAT5 levels of vav-N642H mice[10] (**Figure 1B**). N642H$^{vav/+}$ mice at 8 weeks of age had an elevated BM cellularity and an enlarged hematopoietic stem cell (HSC) pool under homeostatic conditions (**Figure S1C-F**). Numbers of erythroid cells (Ter119$^+$) and NK cells (CD3$^-$NK1.1$^+$) were reduced, while T cells (CD3$^+$CD4$^+$ or CD3$^+$CD8$^+$), B cells (CD19$^+$) and myeloid cells (CD11b$^+$Gr1$^+$) were increased in the BM (**Figure S1G**). At 8 weeks of age, N642H$^{vav/+}$ mice showed splenomegaly (**Figure 1C**) with significantly expanded myeloid and

B-cell compartments (**Figure 1D**). The peripheral blood of N642H$^{vav/+}$ mice lacked any significant alterations in the composition of leukocytes, except for a decrease in the frequency of CD4^{+} T cells (**Figure S1H**).

Upon aging, all N642H$^{vav/+}$ mice developed a hematopoietic malignancy with a median survival of 186 days (**Figure 1E**). The mice suffered from reduced body weight and enlarged spleen and lymph nodes (**Figure 1F+G, S1I+J**). They had significantly elevated numbers of mature hematopoietic cell types in spleen, blood and lymph nodes but not in the BM (**Figure 1G, S1K-M**). Cell numbers were elevated in all lineages and no cell type was dominantly expanded (**Figure 1G, S1K-M**). Blood smears of the diseased N642H$^{vav/+}$ mice showed leukemic blast-like cells (**Figure 1H**). The immune cell infiltration in the lungs was associated with a disruption of the regular lung architecture (**Figure 1I**).

Leukemic N642H$^{vav/+}$ T-/NKT cells expand upon transplantation

To test whether the hematopoietic malignancy is transplantable, we injected Ly5.2^{+} splenic cells of diseased N642H$^{vav/+}$ and healthy aged control mice into immunodeficient NSG recipients (NOD.Cg-Prkdc^{scid} Il2rg^{tm1Wjl}/SzJ). All recipients of N642H$^{vav/+}$ splenocytes developed a disease within 3 months (**Figure 2A**). Ly5.2^{+} N642H$^{vav/+}$ cells densely infiltrated the BM, spleen and lung of the recipients, indicating development of leukemia (**Figure 2B, S2A-C)**. The infiltrating cell types were either T or NKT cells (**Figure 2C+D**). N642H$^{vav/+}$ T and NKT cells expressed almost exclusively TCRβ but not TCRγδ (**Figure 2E+F)**. CD4^{+} and CD8^{+} T/NKT cells expanded in the recipient mice (**Figure 2E+G**). This argues against the idea that a specific T/NKT cell subtype is driving the leukemia. The diseases that develop in N642H$^{vav/+}$ mice closely resemble the T- /NKT-cell diseases observed in patients harboring the *STAT5B^{N642H}* mutation[9].

***STAT5B*^{N642H} promotes cytokine independence of human NK-cell lines**

Despite the presence of an activating STAT5B mutation, N642H$^{vav/+}$ mice did not develop NK-cell leukemia. To investigate the oncogenic potential of STAT5B^{N642H} in NK cells, we ectopically expressed human STAT5B or STATB^{N642H} in two human NK-cell lines (IMC-1 and KHYG-1) that harbor *TP53* mutations but lack mutations in the JAK/STAT3/5 pathway[40,60]. Transduction with STAT5B or STAT5B^{N642H} decreased cell growth in standard IL-2 culture (100U/ml) but gave a growth advantage at limited IL-2 concentrations (25U/ml) (**Figure S3A-F**). In the absence of IL-2, STAT5B^{N642H} was required for cytokine-independent growth (**Figure 3A+B, S3C+F**). This prompted us to test whether STAT5B^{N642H} enhances the

disease-initiating potential of KHYG-1 and IMC-1 cells *in vivo* (**Figure 3C**). When injected into NSG mice, STAT5B^{N642H}-expressing IMC-1 cells accelerated disease onset significantly compared to parental and non-mutant STAT5B-expressing cells (**Figure 3D**). In contrast, neither the parental nor the STAT5B-overexpressing KHYG-1 cells caused disease in NSG recipient mice. All STAT5B^{N642H}-transduced KHYG1 cells induced leukemia within 21-25 days (**Figure 3D**). The disease primarily manifested in the BM and the liver (**Figure 3E-G, S3G**), both typical sites of disease manifestation in NK-cell leukemia patients[11,14,61,62].

An NKp46^{+}-cell specific mouse model to study the oncogenic role of *STAT5B*^{N642H} in NK cells

To investigate the oncogenic role of *STAT5B*^{N642H} in NK cells in detail, we crossed the B6-*Gt(ROSA)26Sor*$^{tm1(STAT5B-N642H)}$ mice to *Ncr1*-iCreTg mice[63] (N642H$^{NK/NK}$). These mice express *STAT5B*^{N642H} exclusively in NKp46^{+} cells, which mainly represent mature NK cells[64,65]. A human *STAT5B* transgene-expressing mouse strain (STAT5B$^{NK/NK}$) and a strain solely expressing eGFP (GFP$^{NK/NK}$) were used as controls (**Figure 4A**). All *Cre*-positive litters expressed GFP in NK cells (**Figure S4A**). We confirmed the V5-tagged transgene expression and elevated STAT5 protein levels in STAT5B$^{NK/NK}$ and N642H$^{NK/NK}$ NK cells compared to GFP$^{NK/NK}$ NK cells (**Figure 4B**).

STAT5B^{N642H} molecules have an enhanced capacity for self-dimerization and a reduced susceptibility to inactivation by dephosphorylation[9]. Compared to STAT5B$^{NK/NK}$ NK cells, N642H$^{NK/NK}$ splenic NK cells displayed enhanced pYSTAT5 levels *ex vivo* already in an unstimulated state and more pronounced after IL-15 stimulation (**Figure S4C+D**). Elevated pYSTAT5 levels were also observed *in vitro* in IL-2 cultured N642H$^{NK/NK}$ splenic NK cells (**Figure 4B, S4B**). Upon cytokine withdrawal, pYSTAT5 dephosphorylation was delayed in N642H$^{NK/NK}$ compared to control NK cells (**Figure 4B, S4B-D).**

Adult N642H$^{NK/NK}$ mice show increased NK-cell numbers in blood, spleen and BM (**Figure 4C-E, S4E-G**). Notably, an expansion of NK cells was already detectable in the blood of N642H$^{NK/NK}$ mice as early as 4 weeks of age (**Figure S4H**). Furthermore, N642H$^{NK/NK}$ mice display more mature NK cells in the BM and spleen compared to control strains (**Figure 4F-G, S4I**). Furthermore, *STAT5B*^{N642H} expression in NK cells was associated with increased survival and reduced apoptosis *ex vivo* (**Figure 4H**). The data are consistent with the idea that STAT5B promotes NK-cell survival and maturation[32]. We found enhanced levels of

Granzyme B and Perforin in N642H$^{NK/NK}$ NK cells (**Figure S4J**), supporting the role of STAT5B in regulating the levels of cytolytic molecules[22,23,30,32].

N642H$^{NK/NK}$ mice develop NK-cell leukemia

The oncogenic potential of *STAT5B*^{N642H} in NK cells was assessed by aging of the animals. While the majority of N642H$^{NK/NK}$ mice maintained an indolent expansion of NK cells, around 33% (8/24) developed disease symptoms within 17 months. One STAT5B$^{NK/NK}$ and one Cre negative (neg) control mouse (out of a total of 50 control mice) were sacrificed due to unspecific age-related symptoms without any signs of leukemia after 486 and 518 days, respectively (**Figure 5A**). The diseased N642H$^{NK/NK}$ mice consistently displayed a leukemic phenotype and suffered from significant body weight loss, splenomegaly, and an expansion of GFP$^+$ cells in various organs, including spleen, liver, BM and blood (**Figure 5B+C, S5A+B, Table S1**). NK cells were the predominantly expanded cell type in the spleen of 5 out of 8 diseased N642H$^{NK/NK}$ mice (#1-#5). One of the diseased mice (#8) displayed an expansion of CD3$^+$NK1.1$^+$ γδ T cells, while two other mice (#6,#7) had a predominant expansion of GFP$^+$ cells lacking both NK- and T-cell markers (CD3$^-$ TCR$^-$NK1.1$^-$ NKp46$^-$ cells) (**Figure 5D+E, S5C, Table S1**). Flow cytometric analysis revealed a downregulation of CD11b, CD49b and NKp46 and a partial increase in CD27, CD49a and NKG2D expression in diseased N642H$^{NK/NK}$ NK cells. KLRG1 expression was significantly increased in diseased N642H$^{NK/NK}$ NK cells (**Figure 5F+G, S5D-F**). Similar deregulations were partially observed in NK cells from non-diseased N642H$^{NK/NK}$ mice, which however more closely resembled control NK cells (**Figure 5B+F+G, S5D, Table S1**).

To confirm the expansion of leukemic cells as the disease cause, we transplanted splenic cells from the diseased N642H$^{NK/NK}$ mice (#1-4, #6-8) into NSG mice (**Figure 6A**). Transplantation initiated a fast-progressing leukemia in all recipient mice. The diseased mice suffered from weight loss, hepatosplenomegaly, anemia and multiple organ infiltration. A leukemia with NK-cell phenotype was observed in ~70% of the transplanted mice (**Figure 6B-E, S6A-H, Table S2**). The transplantation of splenocytes from the mouse that had a lethal expansion of CD3$^+$NK1.1$^+$ TCRγδ$^+$ T cells (#8) verified a disease driven by *STAT5B*^{N642H}-expressing γδ T cells. The transplantation of splenic cells with an accumulation of GFP$^+$ CD3$^-$ TCR$^-$NK1.1$^-$ NKp46$^-$ cells (#6 and #7) revealed that the mice suffered more likely from an NK-cell leukemia than an acute leukemia of T-cell origin as there was a pronounced NK1.1$^+$ but not a CD3$^+$ or TCR$^+$ population upon transplantation (**Figure S6A-H**). We observed leukemic blast-like cells in the blood of all diseased recipient mice (**Figure 6F**). To gauge the

potential for immune evasion of the transformed N642H$^{NK/NK}$ NK cells, we performed parallel transplantations into NSG and Ly5.1 mice (**Figure 6G**). The N642H$^{NK/NK}$ leukemic cells incited disease in both NSG and Ly5.1 mice within a similar time frame and comparable organ infiltration (**Figure 6H, S6I-M**). Furthermore, we established stable NK-cell lines from diseased N642H$^{NK/NK}$ mice and tested their cytokine dependency. All tested cell lines exhibited a dependency on IL-2. One cell line (#3) displayed a growth advantage under reduced IL-2 levels (**Figure S6N+O**). In summary, N642H$^{NK/NK}$ mice predominantly develop a transplantable NK-cell leukemia, which evades immune recognition.

Leukemic N642H$^{NK/NK}$ NK cells display molecular features of NK-cell leukemia patients with *STAT5B* GOF mutations

To investigate the transcriptional changes in *STAT5B*^{N642H}-driven NK-cell leukemia, we performed RNA-Seq of *ex vivo* sorted NK cells from the livers of diseased N642H$^{NK/NK}$ and aged non-diseased control (Cre neg, GFP$^{NK/NK}$), STAT5B$^{NK/NK}$ and N642H$^{NK/NK}$ mice, and γδ T cells of the diseased N642H$^{NK/NK}$ mouse #8. Diseased N642H$^{NK/NK}$ NK cells displayed a distinct transcriptional profile (**Figure S7A**). The leukemic γδ T cells (#8) clustered closely to the leukemic NK cells (**Figure S7A**). We identified significant differentially expressed genes (DEGs) in diseased N642H$^{NK/NK}$ NK cells compared to all genotypes (vs. controls: 888 DEGs; vs. STAT5B$^{NK/NK}$: 997 DEGs; vs. non-diseased N642H$^{NK/NK}$: 1038 DEGs) – mainly upregulated (**Figure S7B-C, Table S3**). We focused on the DEGs in NK cells from diseased N642H$^{NK/NK}$ mice vs. controls for further analysis. To test the identified DEGs for similarities to NK-cell leukemia patients with *STAT5B* GOF mutations, we analyzed RNA-Seq data from 64 NK-cell leukemia patients, showing a different transcriptional profile to healthy controls (PBMCs) and other leukemias. We subdivided the NK-cell leukemia patients according to their JAK/STAT mutations: 3 with *STAT5B* GOF mutations[44] (NK-cell leukemia (*STAT5B* GOF)), 18 with *STAT3* mutations (NK-cell leukemia (*STAT3* mut)), 1 with a *JAK1* mutation (NK-cell leukemia (*JAK1* mut)) and 44 without JAK/STAT mutations (NK-cell leukemia) (**Figure 7A**). Comparison of the leukemic mutant *STAT5B*-driven DEGs between mouse (diseased N642H$^{NK/NK}$ vs control) and human (NK-cell leukemia (*STAT5B* GOF) vs. NK-cell leukemia) identified a set of 135 common DEGs (**Figure 7B, Table S4**). Commonly upregulated genes included genes with oncogenic function (e.g. *Rras2*, *Mybl1*) while genes with tumor suppressive and proinflammatory activities were downregulated (e.g. *Tcf4*, *Dusp1*, *Fos*, *Junb*) (**Figure 7C**). Gene set enrichment analysis (GSEA) revealed 13 identical significant HALLMARK pathways in *STAT5B* GOF human and mouse leukemic NK cells

(**Figure 7D**). All pathways were regulated in the same direction in the mouse and human *STAT5B* GOF comparisons. Significantly upregulated pathways were associated with cell cycle progression, while downregulated pathways were associated with apoptosis and inflammatory processes (**Figure 7E, S7D, Table S5**).

Our findings show that leukemic N642H$^{NK/NK}$ NK cells exhibit transcriptional patterns resembling those found in *STAT5B*-mutated human NK-cell leukemia underlining the translational validity of the mouse model.

Discussion

STAT5B is a prominent driver of hematopoietic diseases[18]. The *STAT5B*^{N642H} mutation is primarily found in diseases arising from T/NKT cells[27]. Previously, a vav-STAT5B^{N642H} mouse model was reported to develop an aggressive CD8$^+$ T-cell lymphoma[10]. We now describe a mouse model (N642H$^{vav/+}$ mice, **Figure 1-2**) that develops slowly progressing CD4$^+$, CD8$^+$ T- or NKT-cell leukemia. N642H$^{vav/+}$ mice display lower pYSTAT5 levels than vav-N642H mice. The different pYSTAT5 levels could stem from a difference in transgene expression levels or might reflect the more progressive CD8$^+$ T-cell disease in young vav-N642H mice. Variations in disease type and onset may result from different promoters driving transgene expression (*CAG* vs. *Vav1*). N642H$^{vav/+}$ mice not only develop a CD8$^+$ T-cell leukemia but also display diverse disease phenotypes, making them a closer representation of patients with *STAT5B* GOF mutations[9]. Our mouse model allows for lineage- or tissue-specific transgene expression to study the impact of *STAT5B*^{N642H} in different cellular and disease contexts.

We focused on using the model to decipher STAT5B^{N642H}'s function in NK cells. *STAT5B*^{N642H} expression in NK cells results in hyperactive STAT5B signaling, elevated cell numbers, decreased apoptosis, increased maturation and higher levels of lytic granzymes. The increased count of mature NK cells in 8-12-week-old N642H$^{NK/NK}$ mice, which do not display disease symptoms, is indicative of an indolent NK-LGLL phenotype[66,67]. This finding aligns with the indolent phenotype of CD4$^+$ T- and NK-LGLL patients carrying *STAT5B* mutations[12,44,46]. One third of the N642H$^{NK/NK}$ mice develop an aggressive disease, suggesting that indolent cases of NK-cell malignancies can transform into aggressive phenotypes, as reported in one NK-LGLL patient with a *STAT5B*^{N642H} mutation[11,68].

Restricting STAT5B^{N642H} expression to NKp46$^+$ cells[63] was crucial for the establishment of a STAT5B^{N642H}-driven NK-cell leukemia model, as vav-N642H[10,54] and N642H$^{vav/+}$ mice

develop T-/NKT-cell but not NK-cell leukemia. NKp46 expression marks mature NK cells[64,65] and highlights them as the origin of NK-cell leukemia in N642H$^{NK/NK}$ mice. In line, human indolent and aggressive NK-cell neoplasms display a mature cytotoxic phenotype[1,69]. Limited data prevents the assessment of whether *STAT5B* GOF mutations in NK-cell leukemia patients are acquired in mature NK cells or at earlier developmental stages. In one NK-LGLL patient, STAT5B^{N642H} was detected in both NK cells and a subset of NKT cells[11], indicating its occurrence at a common progenitor state.

In addition to NK-cell leukemia, one N642H$^{NK/NK}$ mouse developed γδ T-cell leukemia, consistent with NKp46 expression on subsets of γδ T cells[70] and the oncogenic potential of *STAT5B*^{N642H} in γδ T cells[9]. Two diseased N642H$^{NK/NK}$ mice showed an expansion of GFP^{+} cells lacking CD3, TCR and NK1.1 expression, indicating an "undifferentiated" leukemia subtype. Aberrant expression of NK-cell markers has been observed in human cases of mature NK-cell malignancies[71,72] and de-differentiation in is a common feature in several tumor types[73].

Our mouse model resembles human disease as demonstrated by comparative transcriptional analysis. The analyzed human NK-cell leukemia cohort included patients with *STAT3* mutations, which occur more frequent than *STAT5B* mutations[33,36,76–83,39,41,43,44,46,68,74,75]. *STAT5B* GOF cases exhibited a unique transcriptional profile distinct from *STAT3* mutant cases. While both STAT3 and STAT5 act as oncogenes in hematopoietic cancers[84–88], *STAT3* mutations in NK-LGLL associate with more symptomatic cases and an expansion of cytotoxic NK cells[46,67,76,80,82]. However, *STAT3* GOF mutations alone cannot induce LGLL in mouse models[89], unlike STAT5B^{N642H}, which represents a potent oncogenic driver[9,10,54]. The scarcity of *STAT5B* mutated cases might relate to a stronger negative feedback regulation. Excessive STAT5 activation by mutations or cytokines can induce cell death or senescence and chronic exposure to STAT5-activating cytokines can have a negative impact on NK cells[90–94]. The initial growth/survival disadvantage observed upon STAT5B^{N642H} overexpression in human NK-cell lines supports this idea (**Figure S3A-F**) and might explain the low prevalence of aggressive leukemia cases in N642H$^{NK/NK}$ mice. Further exploration is necessary to fully grasp the distinct roles of STAT3 and STAT5B mutations in human NK cell leukemia and murine disease models

STAT5B mutations have also been described in EBV-positive NK-cell malignancies, such as ENKL and ANKL[33,36,43,61,95]. Although N642H$^{NK/NK}$ mice do not mimic the contribution of

EBV infection, understanding the involvement of *STAT5B* mutations in NK-cell transformation is relevant for EBV^{+} NK-cell malignancies. Crossing our N642H$^{NK/NK}$ mice with mouse models displaying conditional expression of EBV proteins[96,97] may further elucidate the interaction between EBV infection and *STAT5B* GOF mutations in NK-cell transformation.

Conventional therapies targeting aberrant STAT5B signaling involve JAK inhibitors. Inhibition of JAKs has drawbacks as it affects additional signaling cascades leading to unintended side-effects[98]. Targeting STAT5B directly using specialized STAT inhibitors or proteolysis targeting chimeras remain challenging due to the lack of an enzymatic activity in STAT5B and its structural similarity to other STAT proteins. This underscores the importance of identifying feasible therapeutic targets downstream of mutant STAT5B. Notably, we observed a significant increase in KLRG1 on the surface of leukemic N642H$^{NK/NK}$ NK cells suggesting a potential therapeutic target. Targeting KLRG1 with monoclonal antibodies could selectively deplete malignant clones[99]. Additionally, our findings indicate immune evasion of transplanted leukemic N642H$^{NK/NK}$ cells, highlighting potential therapeutic implications, particularly in the context of immunotherapies being explored in NK-cell malignancies[100].

Overall, our STAT5B^{N642H}-driven NK-cell leukemia mouse model closely mirrors human NK-cell leukemia representing a resource for a better understanding of NK-cell transformation, the transition from indolent to aggressive disease and for exploring novel therapeutic interventions.

Acknowledgements

We thank Sabine Fajmann, Petra Kudweis and Philipp Jodl for experimental support. We thank Michaela Prchal-Murphy for help and administration regarding animal experiments and ethical permits and all animal caretakers for their work. We thank Bettina Wagner, Lill Anderson and

Tina Bernthaler for their help in the generation of the new NK-cell specific STAT5B^{N642H} transgenic mouse model. We thank Stephan Hutter (MLL) for bioinformatics support in the analysis of primary patient samples. We thank the Next Generation Sequencing Facility at Vienna BioCenter Core Facilities (VBCF), member of the Vienna BioCenter (VBC), Austria. This work was funded in part by the Austrian Science Fund (FWF) Special Research Program SFB-F6107 (grant DOI: 10.55776/F61), the PhD program "Inflammation and Immunity" FWF W1212, Austrian Academy of Sciences doc.funds DOC 32-B28 (grant DOI: 10.55776/DOC32) and the FWF ZK-81B (grant DOI: 10.55776/ZK81). For open access purposes, the author has applied a CC BY public copyright license to any author-accepted manuscript version arising from this submission. The work was also supported by the Fellinger Cancer Research association, the City of Vienna (Stadt Wien Kultur) MA7 Grant, the Lower Austria Research Promotion Agency (Gesellschaft fuer Forschungsfoerderung Niederoesterreich) (grant number GLF21-1-010) and the University of Veterinary Medicine Vienna. K.K. is a recipient of a DOC Fellowship of the Austrian Academy of Sciences at the University of Veterinary Medicine. BioRender.com was used for the graphical illustration of some Figures.

Author Contributions

K.K., V.S. and D.G. conceived the study; T. R. and K.K. generated the mouse model. K.K., S.K., A.H., M.R, J.L., J.T., J.K. and D.G. performed the experiments. K.K., S.K. and D.G. analyzed the data. A.W.S., C.A.B. and B.M. established methods and helped with the experiments and analysis of the data. R.M. and C.G.M. were involved in experimental design and scientific discussions; R.G., T.K., J.K. and S.K analyzed sequencing data; G.H., W.W. and C.G.M. provided bioinformatic patient data analysis; D.G., K.K., S.K., and V.S. wrote the manuscript. D.G. and V.S. provided reagents and supervised the study. All authors revised the manuscript.

Conflict of Interest Disclosures

G.H and W.W: Employment by MLL Munich Leukemia Laboratory; C.G.M. received research funding from Pfizer and AbbVie, is on the Illumina Advisory Board and holds

445 royalties in Cyrus and stocks in Amgen.

446 The authors declare that the research was conducted in the absence of any commercial or

447 financial relationships that could be construed as a potential conflict of interest.

448

References

1. Matutes E. The 2017 WHO update on mature T- and natural killer (NK) cell neoplasms. *Int. J. Lab. Hematol.* 2018;40:97–103.

2. El Hussein S, Medeiros LJ, Khoury JD. Aggressive NK Cell Leukemia: Current State of the Art. *Cancers (Basel).* 2020;12(10):1–16.

3. Sokol L, Loughran TP. Large Granular Lymphocyte Leukemia. *Oncologist*. 2006;11(3):263–273.

4. Nicolae A, Ganapathi KA, Pham THT, et al. EBV-Negative Aggressive NK-Cell Leukemia/Lymphoma: Clinical, Pathological and Genetic Features. *Am. J. Surg. Pathol.* 2017;41(1):67.

5. Koo M, Olevsky O, Ruchalski K, Song S. Primary intestinal NK-cell lymphoma, EBV-negative: A case report and literature review. *Hum. Pathol. Case Reports*. 2019;17:200303.

6. Tang YT, Wang D, Luo H, et al. Aggressive NK-cell leukemia: clinical subtypes, molecular features, and treatment outcomes. *Blood Cancer J. 2017 712*. 2017;7(12):1–5.

7. Stark GR, Darnell JE. The JAK-STAT pathway at twenty. *Immunity*. 2012;36(4):503–14.

8. Sorger H, Dey S, Vieyra-Garcia PA, et al. Blocking STAT3/5 through direct or upstream kinase targeting in leukemic cutaneous T-cell lymphoma. *EMBO Mol. Med.* 2022;14(12):e15200.

9. de Araujo ED, Erdogan F, Neubauer HA, et al. Structural and functional consequences of the STAT5B N642H driver mutation. *Nat. Commun.* 2019;10(1):.

10. Pham HTT, Maurer B, Prchal-Murphy M, et al. STAT5BN642H is a driver mutation for T cell neoplasia. *J. Clin. Invest.* 2018;128(1):387.

11. Rajala HLM, Eldfors S, Kuusanmäki H, et al. Discovery of somatic STAT5b mutations in large granular lymphocytic leukemia. *Blood*. 2013;121(22):4541–50.

12. Andersson EI, Tanahashi T, Sekiguchi N, et al. High incidence of activating STAT5B mutations in CD4-positive T-cell large granular lymphocyte leukemia. *Blood*. 2016;128(20):2465.

13. Bandapalli OR, Schuessele S, Kunz JB, et al. The activating STAT5B N642H mutation is a common abnormality in pediatric T-cell acute lymphoblastic leukemia and confers a higher risk of relapse. *Haematologica*. 2014;99(10):e188-92.

14. Rajala HLM, Porkka K, MacIejewski JP, Loughran TP, Mustjoki S. Uncovering the pathogenesis of large granular lymphocytic leukemia—novel STAT3 and STAT5b mutations. *Ann. Med.* 2014;46(3):114–122.

15. Thomas SJ, Snowden JA, Zeidler MP, Danson SJ. The role of JAK/STAT signalling in the pathogenesis, prognosis and treatment of solid tumours. *Br. J. Cancer*. 2015;113(3):365–371.

16. Pencik J, Pham HTT, Schmoellerl J, et al. JAK-STAT signaling in cancer: From

cytokines to non-coding genome. *Cytokine*. 2016;87:26–36.

17. Berger A, Sexl V, Valent P, Moriggl R. Inhibition of STAT5 : A therapeutic option in BCR-ABL1-driven leukemia. 2014;5(20):9564–9576.

18. Maurer B, Kollmann S, Pickem J, Hoelbl-Kovacic A, Sexl V. STAT5A and STAT5B-Twins with Different Personalities in Hematopoiesis and Leukemia. *Cancers (Basel).* 2019;11(11):.

19. Yu H, Jove R. The STATs of cancer--new molecular targets come of age. *Nat. Rev. Cancer*. 2004;4:97–105.

20. Steelman LS, Pohnert SC, Shelton JG, et al. JAK/STAT, Raf/MEK/ERK, PI3K/Akt and BCR-ABL in cell cycle progression and leukemogenesis. *Leukemia*. 2004;18(2):189–218.

21. Kollmann S, Grausenburger R, Klampfl T, et al. A STAT5B-CD9 axis determines self-renewal in hematopoietic and leukemic stem cells. *Blood*. 2021;138(23):2347–2359.

22. Vargas-Hernández A, Witalisz-Siepracka A, Prchal-Murphy M, et al. Human STAT5b mutation causes dysregulated human natural killer cell maturation and impaired lytic function. *J. Allergy Clin. Immunol.* 2020;145(1):345.

23. Villarino A V., Sciumè G, Davis FP, et al. Subset- and tissue-defined STAT5 thresholds control homeostasis and function of innate lymphoid cells. *J. Exp. Med.* 2017;214(10):2999–3014.

24. Bagger FO, Sasivarevic D, Sohi SH, et al. BloodSpot: a database of gene expression profiles and transcriptional programs for healthy and malignant haematopoiesis. *Nucleic Acids Res.* 2016;44(D1):D917–D924.

25. Kofoed EM, Hwa V, Little B, et al. Growth hormone insensitivity associated with a STAT5b mutation. *N. Engl. J. Med.* 2003;349(12):1139–47.

26. Bezrodnik L, Di Giovanni D, Caldirola MS, et al. Long-Term Follow-up of STAT5B Deficiency in Three Argentinian Patients: Clinical and Immunological Features. *J. Clin. Immunol.* 2015;35(3):264–272.

27. Hwa V. STAT5B deficiency: Impacts on human growth and immunity. *Growth Horm. IGF Res.* 2016;28:16–20.

28. Kanai T, Jenks J, nadeau KC. The STAT5b Pathway Defect and Autoimmunity. *Front. Immunol.* 2012;3:234.

29. Bernasconi A, Marino R, Ribas A, et al. Characterization of immunodeficiency in a patient with growth hormone insensitivity secondary to a novel STAT5b gene mutation. *Pediatrics*. 2006;118(5):.

30. Imada K, Bloom ET, Nakajima H, et al. Stat5b is essential for natural killer cell-mediated proliferation and cytolytic activity. *J Exp Med*. 1998;188(11):2067–2074.

31. Villarino A, Laurence A, Robinson GW, et al. Signal transducer and activator of transcription 5 (STAT5) paralog dose governs T cell effector and regulatory functions. *Elife*. 2016;5(MARCH2016):.

32. Gotthardt D, Putz EM, Grundschober E, et al. STAT5 Is a Key Regulator in NK Cells and Acts as a Molecular Switch from Tumor Surveillance to Tumor Promotion. *Cancer*

Discov. 2016;6(4):414–29.

33. Song TL, Nairismägi ML, Laurensia Y, et al. Oncogenic activation of the STAT3 pathway drives PD-L1 expression in natural killer/T-cell lymphoma. *Blood*. 2018;132(11):1146–1158.

34. Nicolae A, Xi L, Pittaluga S, et al. Frequent STAT5B mutations in γδ hepatosplenic T-cell lymphomas. *Leuk. 2014 2811*. 2014;28(11):2244–2248.

35. McKinney M, Moffitt AB, Gaulard P, et al. The Genetic Basis of Hepatosplenic T-cell Lymphoma. *Cancer Discov.* 2017;7(4):369–379.

36. Huang L, Liu D, Wang N, et al. Integrated genomic analysis identifies deregulated JAK/STAT-MYC-biosynthesis axis in aggressive NK-cell leukemia. *Cell Res. 2018 282*. 2017;28(2):172–186.

37. Kiel MJ, Velusamy T, Rolland D, et al. Integrated genomic sequencing reveals mutational landscape of T-cell prolymphocytic leukemia. *Blood*. 2014;124(9):1460–72.

38. Kiel MJ, Sahasrabuddhe AA, Rolland DCM, et al. Genomic analyses reveal recurrent mutations in epigenetic modifiers and the JAK–STAT pathway in Sézary syndrome. *Nat. Commun. 2015 61*. 2015;6(1):1–10.

39. Dufva O, Kankainen M, Kelkka T, et al. Aggressive natural killer-cell leukemia mutational landscape and drug profiling highlight JAK-STAT signaling as therapeutic target. *Nat. Commun.* 2018;

40. Gao LM, Zhao S, Liu WP, et al. Clinicopathologic characterization of aggressive natural killer cell leukemia involving different tissue sites. *Am. J. Surg. Pathol.* 2016;40(6):836–846.

41. Jiang L, Gu Z, Yan Z, et al. Exome sequencing identifies somatic mutations of DDX3X in natural killer / T-cell lymphoma. 2015;47(9):.

42. Kontro M, Kuusanmäki H, Eldfors S, et al. Novel activating STAT5B mutations as putative drivers of T-cell acute lymphoblastic leukemia. *Leukemia*. 2014;28(8):1738–42.

43. Küçük C, Jiang B, Hu X, et al. Activating mutations of STAT5B and STAT3 in lymphomas derived from γδ-T or NK cells. *Nat. Commun.* 2015;6:6025.

44. Baer C, Kimura S, Rana MS, et al. CCL22 mutations drive natural killer cell lymphoproliferative disease by deregulating microenvironmental crosstalk. *Nat. Genet.* 2022;54(5):637.

45. Xiong J, Cui BW, Wang N, et al. Genomic and Transcriptomic Characterization of Natural Killer T Cell Lymphoma. *Cancer Cell*. 2020;37(3):403-419.e6.

46. Pastoret C, Desmots F, Drillet G, et al. Linking the KIR phenotype with STAT3 and TET2 mutations to identify chronic lymphoproliferative disorders of NK cells. *Blood*. 2021;137(23):3237.

47. Waldmann TA, Chen J. Disorders of the JAK/STAT Pathway in T Cell Lymphoma Pathogenesis: Implications for Immunotherapy. *Annu. Rev. Immunol.* 2017;35:533–550.

48. Wu Y, Tian Z, Wei H. Developmental and functional control of natural killer cells by

cytokines. *Front. Immunol.* 2017;8(AUG):271745.

49. Rani A, Murphy JJ. STAT5 in Cancer and Immunity. *J. Interferon Cytokine Res.* 2016;36(4):226–237.

50. Yokohama A, Mishra A, Mitsui T, et al. A novel mouse model for the aggressive variant of NK cell and T cell large granular lymphocyte leukemia. *Leuk. Res.* 2010;34(2):203.

51. Fehniger TA, Suzuki K, VanDeusen JB, et al. Fatal Leukemia in Interleukin-15 Transgenic Mice. *Blood Cells, Mol. Dis.* 2001;27(1):223–230.

52. Fehniger TA, Suzuki K, Ponnappan A, et al. Fatal leukemia in interleukin 15 transgenic mice follows early expansions in natural killer and memory phenotype CD8+ T cells. *J. Exp. Med.* 2001;193(2):219–231.

53. Sato N, Sabzevari H, Fu S, et al. Development of an IL-15–autocrine CD8 T-cell leukemia in IL-15–transgenic mice requires the cis expression of IL-15Rα. *Blood*. 2011;117(15):4032.

54. Klein K, Witalisz-Siepracka A, Maurer B, et al. STAT5BN642H drives transformation of NKT cells: a novel mouse model for CD56+ T-LGL leukemia. *Leukemia*. 2019;33(9):2336–2340.

55. Belgardt BF, Husch A, Rother E, et al. PDK1 Deficiency in POMC-Expressing Cells Reveals FOXO1-Dependent and -Independent Pathways in Control of Energy Homeostasis and Stress Response. *Cell Metab.* 2008;7(4):291–301.

56. Hagemann-Jensen M, Ziegenhain C, Chen P, et al. Single-cell RNA counting at allele and isoform resolution using Smart-seq3. *Nat. Biotechnol.* 2020;38(6):708–714.

57. Babraham Bioinformatics - FastQC A Quality Control tool for High Throughput Sequence Data.

58. Stengel A, Shahswar R, Haferlach T, et al. Whole transcriptome sequencing detects a large number of novel fusion transcripts in patients with AML and MDS. *Blood Adv.* 2020;4(21):5393–5401.

59. Ogilvy S, Metcalf D, Gibson L, et al. Promoter Elements of vav Drive Transgene Expression In Vivo Throughout the Hematopoietic Compartment. *Blood*. 1999;94(6):1855–1863.

60. Parri E, Kuusanmäki H, Bulanova D, Mustjoki S, Wennerberg K. Selective drug combination vulnerabilities in STAT3- and TP53-mutant malignant NK cells. *Blood Adv.* 2021;5(7):1862–1875.

61. Gao LM, Zhao S, Liu WP, et al. Clinicopathologic Characterization of Aggressive Natural Killer Cell Leukemia Involving Different Tissue Sites. *Am. J. Surg. Pathol.* 2016;40(6):836–846.

62. Kameda K, Yanagiya R, Miyatake Y, et al. The hepatic niche leads to aggressive natural killer cell leukemia proliferation through the transferrin–transferrin receptor 1 axis. *Blood*. 2023;142(4):352–364.

63. Eckelhart E, Warsch W, Zebedin E, et al. A novel Ncr1-Cre mouse reveals the essential role of STAT5 for NK cell survival and development. *Blood*. 2011;117(5):1565–73.

64. Gotthardt D, Prchal-Murphy M, Seillet C, et al. NK cell development in bone marrow and liver: site matters. *Genes Immun.* 2014;15(8):584–7.

65. Ma S, Caligiuri MA, Yu J. A four-stage model for murine natural killer cell development in vivo. *J. Hematol. Oncol.* 2022;15(1):1–5.

66. Poullot E, Zambello R, Leblanc F, et al. Chronic natural killer lymphoproliferative disorders: characteristics of an international cohort of 70 patients. *Ann. Oncol.* 2014;25(10):2030.

67. Kurt H, Jorgensen JL, Amin HM, et al. Chronic lymphoproliferative disorder of NK-cells: A single-institution review with emphasis on relative utility of multimodality diagnostic tools. *Eur. J. Haematol.* 2018;100(5):444–454.

68. Gasparini VR, Binatti A, Coppe A, et al. A high definition picture of somatic mutations in chronic lymphoproliferative disorder of natural killer cells. *Blood Cancer J. 2020 104*. 2020;10(4):1–11.

69. Alaggio R, Amador C, Anagnostopoulos I, et al. The 5th edition of the World Health Organization Classification of Haematolymphoid Tumours: Lymphoid Neoplasms. *Leukemia*. 2022;36(7):1720–1748.

70. Walzer T, Bléry M, Chaix J, et al. Identification, activation, and selective in vivo ablation of mouse NK cells via NKp46. *Proc. Natl. Acad. Sci. U. S. A.* 2007;104(9):3384–3389.

71. Yang J, Li P, Piao Y, et al. CD56-Negative Extranodal Natural Killer/T-Cell Lymphoma: A Retrospective Study in 443 Patients Treated by Chemotherapy With or Without Asparaginase. *Front. Immunol.* 2022;13:829366.

72. Guerreiro M, Príncipe F, Teles MJ, et al. CD56-Negative Aggressive NK Cell Leukemia Relapsing as Multiple Cranial Nerve Palsies: Case Report and Literature Review. *Case Rep. Hematol.* 2017;2017:1–9.

73. Li J, Stanger BZ. How Tumor Cell Dedifferentiation Drives Immune Evasion And Resistance to Immunotherapy. *Cancer Res.* 2020;80(19):4037.

74. Ishida F. Aggressive NK-cell leukemia. *Front. Pediatr.* 2018;6:292.

75. Jerez A, Clemente MJ, Makishima H, et al. STAT3 mutations unify the pathogenesis of chronic lymphoproliferative disorders of NK cells and T cell large granular lymphocyte leukemia. *Blood*. 2012;120(15):3048–3058.

76. Kawakami T, Sekiguchi N, Kobayashi J, et al. STAT3 mutations in natural killer cells are associated with cytopenia in patients with chronic lymphoproliferative disorder of natural killer cells. *Int. J. Hematol.* 2019;109(5):563–571.

77. Fasan A, Kern W, Haferlach C, Haferlach T, Schnittger S. STAT3 Mutations in Large Granular Lymphocytic Leukemia. *Blood*. 2012;120(21):1606.

78. Lee S, Park HY, Kang SY, et al. Genetic alterations of JAK/STAT cascade and histone modification in extranodal NK/T-cell lymphoma nasal type. *Oncotarget*. 2015;6(19):17764.

79. Tse E, Kwong YL. The diagnosis and management of NK/T-cell lymphomas. *J. Hematol. Oncol.* 2017;10(1):.

80. Barilà G, Calabretto G, Teramo A, et al. T cell large granular lymphocyte leukemia and chronic NK lymphocytosis. *Best Pract. Res. Clin. Haematol.* 2019;32(3):207–216.

81. Barilà G, Teramo A, Calabretto G, et al. Stat3 mutations impact on overall survival in large granular lymphocyte leukemia: a single-center experience of 205 patients. *Leukemia*. 2020;34(4):1116–1124.

82. Olson TL, Cheon HJ, Xing JC, et al. Frequent somatic TET2 mutations in chronic NK-LGL leukemia with distinct patterns of cytopenias. *Blood*. 2021;138(8):662–673.

83. Teramo A, Barilà G, Calabretto G, et al. Insights Into Genetic Landscape of Large Granular Lymphocyte Leukemia. *Front. Oncol.* 2020;10:.

84. Wingelhofer B, Maurer B, Heyes EC, et al. Pharmacologic inhibition of STAT5 in acute myeloid leukemia. *Leukemia*. 2018;32(5):1135.

85. Orlova A, Wagner C, De Araujo ED, et al. Direct Targeting Options for STAT3 and STAT5 in Cancer. *Cancers (Basel).* 2019;11(12):.

86. Brachet-Botineau M, Deynoux M, Vallet N, et al. A Novel Inhibitor of STAT5 Signaling Overcomes Chemotherapy Resistance in Myeloid Leukemia Cells. *Cancers (Basel).* 2019;11(12):.

87. Igelmann S, Neubauer HA, Ferbeyre G. STAT3 and STAT5 Activation in Solid Cancers. *Cancers (Basel).* 2019;11(10):.

88. Verhoeven Y, Tilborghs S, Jacobs J, et al. The potential and controversy of targeting STAT family members in cancer. *Semin. Cancer Biol.* 2020;60:41–56.

89. Dutta A, Yan D, Hutchison RE, Mohi G. STAT3 mutations are not sufficient to induce large granular lymphocytic leukaemia in mice. *Br. J. Haematol.* 2018;180(6):911–915.

90. Felices M, Lenvik AJ, McElmurry R, et al. Continuous treatment with IL-15 exhausts human NK cells via a metabolic defect. *JCI insight*. 2018;3(3):.

91. Alvarez M, Simonetta F, Baker J, et al. Regulation of murine NK cell exhaustion through the activation of the DNA damage repair pathway. *JCI insight*. 2019;5(14):.

92. Elpek KG, Rubinstein MP, Bellemare-Pelletier A, Goldrath AW, Turley SJ. Mature natural killer cells with phenotypic and functional alterations accumulate upon sustained stimulation with IL-15/IL-15Rα complexes. *Proc. Natl. Acad. Sci. U. S. A.* 2010;107(50):21647–21652.

93. Mallette FA, Gaumont-Leclerc MF, Ferbeyre G. The DNA damage signaling pathway is a critical mediator of oncogene-induced senescence. *Genes Dev.* 2007;21(1):43–48.

94. Epling-Burnette PK, Liu JH, Catlett-Falcone R, et al. Inhibition of STAT3 signaling leads to apoptosis of leukemic large granular lymphocytes and decreased Mcl-1 expression. *J. Clin. Invest.* 2001;107(3):351–361.

95. Jiang L, Gu Z-H, Yan Z-X, et al. Exome sequencing identifies somatic mutations of DDX3X in natural killer/T-cell lymphoma. *Nat. Genet.* 2015;47(9):1061–1066.

96. Wirtz S, Neufert C, Weigmann B, Neurath MF. Chemically induced mouse models of intestinal inflammation. *Nat. Protoc.* 2007;2(3):541–546.

97. Zhang B, Kracker S, Yasuda T, et al. Immune surveillance and therapy of lymphomas

693 driven by Epstein-Barr virus protein LMP1 in a mouse model. *Cell*. 2012;148(4):739–
694 751.

695 98. Shawky AM, Almalki FA, Abdalla AN, Abdelazeem AH, Gouda AM. A
696 Comprehensive Overview of Globally Approved JAK Inhibitors. *Pharmaceutics*.
697 2022;14(5):.

698 99. Assatova B, Willim R, Trevisani C, et al. KLRG1 Cell Depletion As A Novel
699 Therapeutic Strategy In Patients With Mature T-cell lymphoma Subtypes. *Clin. Cancer*
700 *Res.* 2024;

701 100. He L, Chen N, Dai L, Peng X. Advances and challenges of immunotherapies in NK/T
702 cell lymphomas. *iScience*. 2023;26(11):.

703

704

Figure Legends

Figure 1. N642H$^{vav/+}$ mice develop a hematopoietic malignancy

(A) Schematic overview of the generation of N642H$^{vav/+}$ mice (B) (*Left*) V5, pYSTAT5 and STAT5A/B immunoblot analysis of BM cells from vav-N642H (n=1), N642H$^{vav/+}$ (n=4) and control (N642H$^{STOP/+}$) mice (n=4). α-TUBULIN served as loading control. (*Right*) Quantification of fold change (fc) of pYSTAT5 relative to total STAT5A/B levels, based on immunoblot analysis, from 8-week-old control and N642H$^{vav/+}$ BM cells (n=4/genotype, mean±SD). (C) Relative quantification of spleen weights from 8-week-old control and N642H$^{vav/+}$ mice (n=4/genotype, mean±SD). (D) (*Left*) Relative quantification (percentages out of living cells) and (*Right*) total numbers of myeloid cells (CD11b$^+$Gr1$^+$), B cells (CD19$^+$), CD4$^+$ T cells (CD3$^+$CD4$^+$), CD8$^+$ T cells (CD3$^+$CD8$^+$) and NK cells (CD3$^-$NK1.1$^+$) in the spleen of 8-week-old control and N642H$^{vav/+}$ mice (n=4/genotype, mean±SD). (E) Survival analysis of aged N642H$^{vav/+}$ (142-363 days of survival) and control mice (n≥5/genotype). (F) Representative pictures of spleens and LNs of (*Left*) aged control and (*Right*) diseased N642H$^{vav/+}$ mice. (G) (*Left*) Relative quantification and (*Right*) total numbers of myeloid cells (CD11b$^+$Gr1$^+$), B cells (CD19$^+$), CD4$^+$ T cells (CD3$^+$CD4$^+$), CD8$^+$ T cells (CD3$^+$CD8$^+$) and NK cells (CD3$^-$NK1.1$^+$) in the spleen of aged control (~360 days old) and diseased N642H$^{vav/+}$ mice (endpoint analysis) (n≥5/genotype, mean±SD). (H) Hemacolor® Rapid staining of blood smears from control and diseased N642H$^{vav/+}$ mice (one representative picture/genotype). (I) H&E staining of lung tissue from control and diseased N642H$^{vav/+}$ mice (one representative picture/genotype).

Levels of significance were calculated using unpaired t-test in (B) - (D) and (G) and Mantel-Cox text in (E). *p < 0.05, **p < 0.01, ***p < 0.001 and ****p < 0.0001.

Figure 2. Leukemic N642H$^{vav/+}$ T-/NKT cells expand upon transplantation

Splenic cells (Ly5.2$^+$) from either aged control or diseased N642H$^{vav/+}$ mice were intravenously (*i.v.*) injected into NSG mice and analyzed. (A) Survival analysis (n≥4/genotype). (B) Quantification of GFP levels among transplanted Ly5.2$^+$ cells in BM, spleen and lung of NSG mice injected with control or N642H$^{vav/+}$ cells (n≥3/genotype, mean±SD). (C) Quantification of the leukemia type developed in the N642H$^{vav/+}$ transplanted NSG recipients. (D) Relative quantification (percentages out of injected Ly5.2$^+$ N642H$^{vav/+}$ cells) of N642H$^{vav/+}$ myeloid cells (CD11b$^+$Gr1$^+$), B cells (CD19$^+$), T cells (CD3$^+$NK1.1$^-$), NKT cells (CD3$^+$NK1.1$^+$) and NK cells (CD3$^-$NK1.1$^+$) in BM, lung and spleen of four to five

of the diseased N642H$^{vav/+}$ transplanted NSG mice. (E) Representative FACS plots of TCRβ and TCRγδ gating starting from Ly5.2+ T cells (CD3$^+$NK1.1$^-$) or NKT cells (CD3$^+$NK1.1$^+$) in BM of N642H$^{vav/+}$ transplanted NSG mice. (F) Relative quantification of TCRβ or TCRγδ expression on tranplanted Ly5.2$^+$ N642H$^{vav/+}$ T cells (CD3$^+$NK1.1$^-$) or NKT cells (CD3$^+$NK1.1$^+$) (n≥4). (G) Relative quantification of CD4 or CD8 expression on transplanted Ly5.2$^+$TCRβ$^+$CD3$^+$NK1.1$^-$ or Ly5.2$^+$ TCRβ$^+$CD3$^+$NK1.1$^+$ N642H$^{vav/+}$ cells (n≥4).

Levels of significance were calculated using Mantel-Cox text in (A) and Mann-Whitney test in (B). *p < 0.05 and **p < 0.01.

Figure 3. *STAT5B^{N642H}* promotes cytokine independence of leukemic human NK cells

(A) IMC-1 and (B) KHYG-1 cell lines were transduced with non-mutant STAT5B (+STAT5B) or STAT5B^{N642H} (+STAT5B^{N642H}). As a control, cells were transduced with the empty vector, carrying only IRES-controlled eGFP (+GFP). After initial culture in presence of IL-2, transduced cells were completely deprived of IL-2. The percentage of transduced (GFP$^+$) cells depicted as $\log_2$ fc relative to day 0 was monitored over time after cytokine withdrawal. (C) Schematic overview for transplantation of cytokine-independent STAT5B^{N642H} transduced, IL-2 dependent non-mutant STAT5B transduced and non-transduced IMC-1 and KHYG-1 cells into immunodeficient NSG mice. (D) Survival analysis of (*Left*) IMC-1 and (*Right*) KHYG-1 transplanted NSG mice (n≥3/cell line). (E) Relative quantification (percentages out of living cells) of non-mutant STAT5B or STAT5B^{N642H} transduced (GFP$^+$) cells in blood, spleen, liver and BM of transplanted NSG mice (n≥2/genotype, mean±SD). (F) Representative histograms for GFP signal within living cells in the (*Left*) liver and (*Right*) BM of transplanted NSG mice. (G) Representative images of H&E-stained liver and BM tissue from untransplanted (no NK) NSG mice and NSG mice transplanted with non-mutant STAT5B (KHYG1 + STAT5B) or STAT5B^{N642H} transduced KHYG-1 cells (KHYG1 + STAT5B^{N642H}).

Levels of significance were calculated using Mantel-Cox text in (D) and Mann-Whitney test in (E). *p < 0.05, **p < 0.01, ***p < 0.001, ****p < 0.0001.

Figure 4. An NKp46$^+$-cell specific mouse model to study the oncogenic role of *STAT5B*^{N642H} in NK cells

(A) Schematic overview of the generation of N642H$^{NK/NK}$, STAT5B$^{NK/NK}$ and GFP$^{NK/NK}$ mice. (B) pYSTAT5, STAT5A/B and V5 immunoblot analysis of IL-2 cultured NK cells from

GFP$^{NK/NK}$, STAT5B$^{NK/NK}$ and N642H$^{NK/NK}$ mice. IL-2 cultured NK cells were either directly lysed (+IL-2), lysed after being starved off IL-2 for 3h (starv.) or lysed after IL-2 starvation and restimulation with IL-2 and IL-15 (restim.). β-Actin served as a loading control. Absolute numbers of NK cells (CD3$^-$NK1.1$^+$NKp46$^+$) in (C) blood and (D) spleen of 8-12-week-old GFP$^{NK/NK}$, STAT5B$^{NK/NK}$, N642H$^{NK/NK}$ and Cre negative (neg) control mice (n≥5/genotype, mean±SD). (E) Absolute numbers of NK cells (lineage (Lin) negative (CD3$^-$CD19$^-$Gr1$^-$ Ter119$^-$) CD122$^+$ cells) in BM of 8-12-week-old GFP$^{NK/NK}$, STAT5B$^{NK/NK}$, N642H$^{NK/NK}$ and Cre neg mice (n≥6/genotype, mean±SD). (F) *(Left*) Representative gating of NK-cell developmental stages among Lin-CD122$^+$ cells within the BM, including NK1.1$^-$NKp46$^-$ NK cell precursors (NKPs), NK1.1$^+$NKp46$^-$ immature (iNKs) and NK1.1$^+$NKp46$^+$ mature NK cells (mNKs). *(Right)* Percentages of NKPs, iNKs and mNKs among Lin$^-$CD122$^+$ BM cells (n≥6/genotype, mean±SD). (G) *(Left*) Schematic overview on splenic NK-cell maturation stages based on CD27 and CD11b expression. *(Right)* Percentages of CD27$^+$CD11b$^-$, CD27$^+$CD11b$^+$ and CD27$^-$CD11b$^+$ NK cells in the spleens of GFP$^{NK/NK}$, STAT5B$^{NK/NK}$, N642H$^{NK/NK}$ and Cre neg mice (n≥6/genotype, mean±SD). (H) Apoptosis staining of splenic NK cells from GFP$^{NK/NK}$, STAT5B$^{NK/NK}$, N642H$^{NK/NK}$ and Cre neg mice (n≥4/genotype, mean±SD).

Levels of significance were calculated using one-way ANOVA in (C) – (H). *p < 0.05, **p < 0.01, ***p < 0.001, ****p < 0.0001.

Figure 5. *STAT5B*^{N642H} induces NK-cell leukemia in mice

Cre neg, GFP$^{NK/NK}$, STAT5B$^{NK/NK}$ and N642H$^{NK/NK}$ mice were aged and monitored for signs of disease development. (A) Survival analysis of Cre neg, GFP$^{NK/NK}$, STAT5B$^{NK/NK}$ and N642H$^{NK/NK}$ mice (n≥12/genotype). (B) Flow cytometric analysis of GFP$^+$ cells in different tissues of Cre neg, GFP$^{NK/NK}$, STAT5B$^{NK/NK}$, non-diseased N642H$^{NK/NK}$ and diseased N642H$^{NK/NK}$ mice (n≥8/group, mean±SD). (C) Body weight quantification of Cre neg, GFP$^{NK/NK}$, STAT5B$^{NK/NK}$, non-diseased N642H$^{NK/NK}$ and diseased N642H$^{NK/NK}$ mice (n≥8/group, mean±SD). (D) Quantification of the leukemia type developed by N642H$^{NK/NK}$ mice. (E) Relative quantification of CD3$^+$NK1.1$^-$ T cells, CD3$^+$NK1.1$^+$ NKT cells, CD3$^-$ NK1.1$^+$ NK cells and CD3$^-$NK1.1$^-$ "undifferentiated" cells among GFP$^+$ cells in the spleen of diseased N642H$^{NK/NK}$ mice (n=8). (F) Flow cytometric analysis of GFP$^+$ cells in the liver of Cre neg, GFP$^{NK/NK}$, STAT5B$^{NK/NK}$, non-diseased N642H$^{NK/NK}$ and diseased N642H$^{NK/NK}$ mice (n≥8/group, mean±SD). Heatmap depicts percentage of GFP$^+$ cells out of living cells, percentages of DN (double-negative, CD27$^-$CD11b$^-$), CD27$^+$, DP (double-positive,

CD27$^+$CD11b$^+$), CD11b$^+$, CD49a$^+$, CD49b$^+$ and KLRG1$^+$ cells out of GFP$^+$ NK cells (CD3$^-$ NK1.1$^+$) and median fluorescence intensity (MFI) of NKp46, KLRG1 and NKG2D on GFP$^+$ NK cells. (G) *(Left*) Percentages of KLRG1$^+$ and *(right*) MFI of KLRG1 on GFP$^+$ NK cells in the spleen and liver of Cre neg, GFP$^{NK/NK}$, STAT5B$^{NK/NK}$, non-diseased N642H$^{NK/NK}$ and diseased N642H$^{NK/NK}$ mice (n≥8/group, mean±SD).

Levels of significance were calculated using Mantel-Cox test in (A) and one-way ANOVA in (B), (C) and (G). *p < 0.05, **p < 0.01, ***p < 0.001, ****p < 0.0001.

Figure 6. *STAT5B*^{N642H} induces transplantable NK-cell leukemia in mice

(A) Schematic overview of the *i.v.* transplantation of splenocytes from diseased N642H$^{NK/NK}$ mice into NSG mice. (B) Survival analysis of NSG mice transplanted with splenocytes of diseased N642H$^{NK/NK}$ mice (#1-4 and #6-8) (n=7). (C) Quantification of (*left*) body weight, (*middle*) spleen to body weight ratio and (*right*) liver to body weight ratio of diseased N642H$^{NK/NK}$ transplanted NSG mice and untransplanted controls (n≥4/group, mean±SD). (D) Flow cytometric analysis of GFP$^+$ cells in different tissues of NSG mice transplanted with splenocytes from the different diseased N642H$^{NK/NK}$ mice (1st transplant). (E) Quantification of the leukemia type developed by NSG recipients of diseased N642H$^{NK/NK}$ splenocytes. (F) Representative images of H&E-stained blood smears from NSG mice transplanted with splenocytes from diseased N642H$^{NK/NK}$ mouse (*left*) #7 and (*right*) #3. (G) Schematic overview of the *i.v.* transplantation of splenocytes from diseased N642H$^{NK/NK}$ transplanted NSG mice into another round of NSG recipients or immunocompetent WT (Ly5.1$^+$) mice (2nd transplant). (H) Survival analysis of N642H$^{NK/NK}$ transplanted NSG and Ly5.1 recipients (n=4/group).

Levels of significance were calculated using unpaired t-test in (C). *p < 0.05, **p < 0.01.

Figure 7. Leukemic N642H$^{NK/NK}$ NK cells display molecular features of NK-cell leukemia patients harboring *STAT5B* GOF mutations

RNA-sequencing data of NK cells from Cre neg, GFP$^{NK/NK}$, STAT5B$^{NK/NK}$, non-diseased and diseased N642H$^{NK/NK}$ mice and NK-cell leukemia patients. (A) Principal component analysis of RNA-sequencing data of control (PBMC), B-cell precursor acute lymphoblastic leukemia (BCP-ALL), T-cell acute lymphoblastic leukemia (T-ALL), NK-cell leukemia patients: without *JAK/STAT* mutations (NK-cell leukemia, n=44), with mutated *STAT3* (NK-cell leukemia (*STAT3* mut), n=16), with mutated *JAK1* (NK-cell leukemia (*JAK1* mut), n=1), or with *STAT5B* GOF mutations (NK-cell leukemia (*STAT5B* GOF), n=3). One *STAT5B* GOF

patient harbors a *STAT5B*^{N642H}, one a *STAT5B*^{Q706L}, and one patient harbors a *STAT5B*^{Y665F} and a *STAT5B*^{V712E} co-mutation. (B) Venn diagram illustrating common DEGs from the comparisons diseased N642H$^{NK/NK}$ (n=8) vs. control (GFP$^{NK/NK}$ or Cre neg mice; n=5) (adjusted p-value < 0.1) and NK-cell leukemia (*STAT5B* GOF) (n=3) vs. NK-cell leukemia (n=44) (FDR < 0.1). This analysis considered exclusively DEGs with available human-mouse orthologues. (C) Heatmap illustrating expression of the commonly regulated DEGs from the comparisons: diseased N642H$^{NK/NK}$ (n=8) vs. control (n=5) and NK-cell leukemia (*STAT5B* GOF) (n=3) vs. NK-cell leukemia (n=44). (D) Venn diagram illustrating significant (FDR<0.1) HALLMARK pathways from the comparisons diseased N642H$^{NK/NK}$ (n=8) vs. control (n=5) and NK-cell leukemia (*STAT5B* GOF) (n=3) vs. NK-cell leukemia (n=44). (E) Quantification of the normalized enrichment score (NES) of the 13 common HALLMARK pathways identified in (D).

Figure 1: N642H$^{vav/+}$ mice develop a hematopoietic malignancy

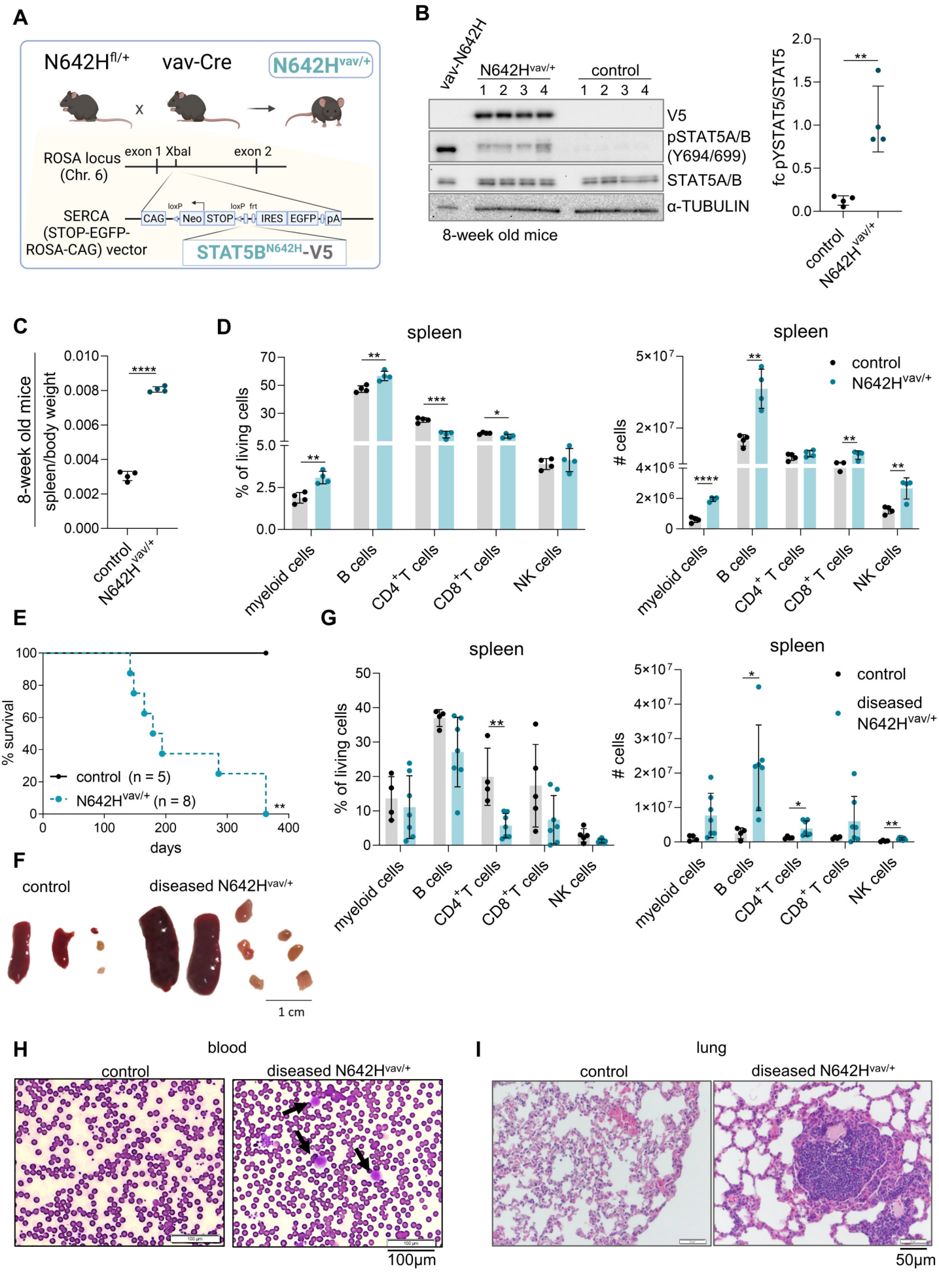

Figure 2: Leukemic N642H$^{vav/+}$ T-/NKT cells expand upon transplantation

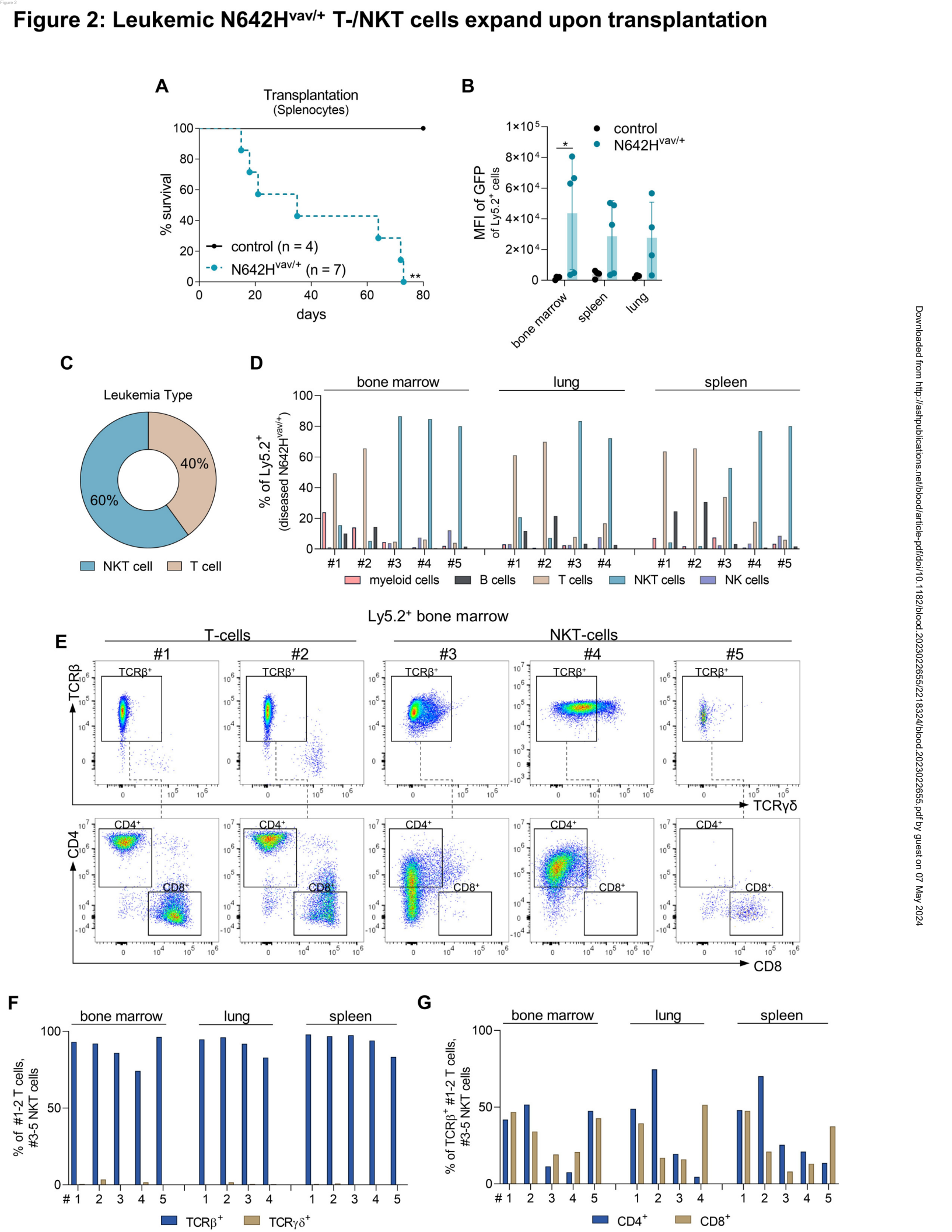

Figure 3: *STAT5B*^{N642H} promotes cytokine independence of leukemic human NK cells

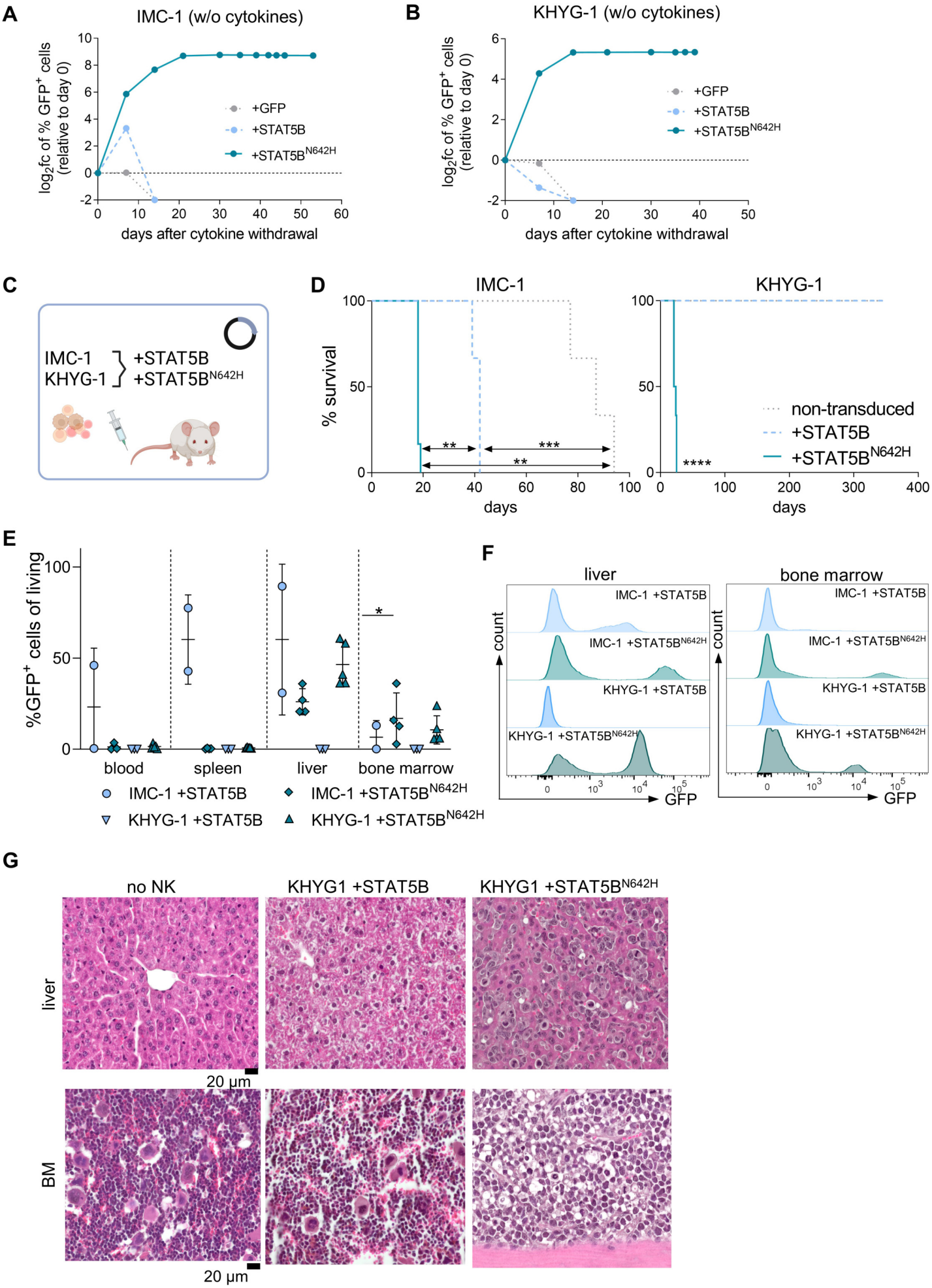

Figure 4

Figure 4: An NKp46^{+}-cell specific mouse model to study the oncogenic role of *STAT5B*^{N642H} in NK cells

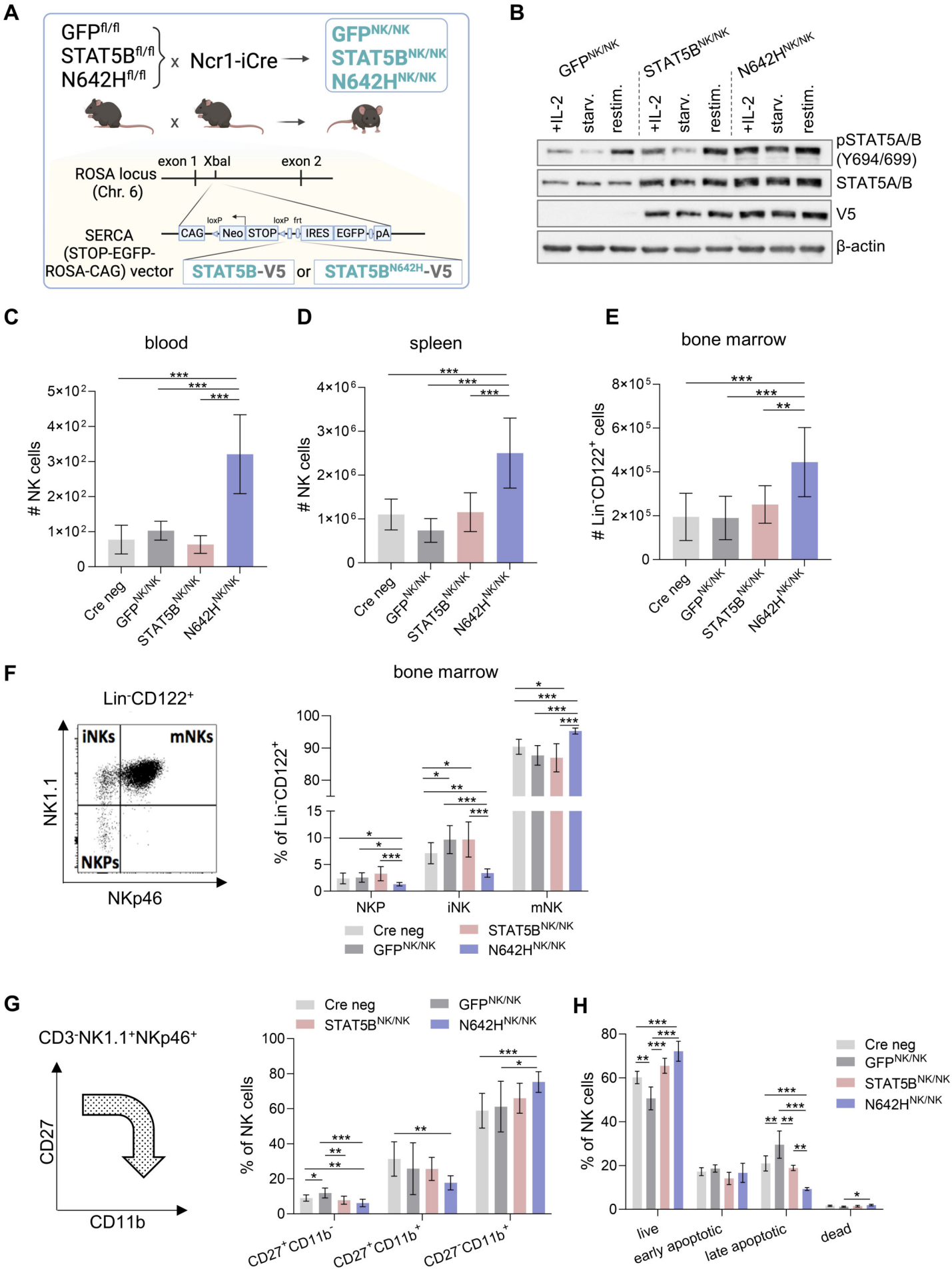

Figure 5: *STAT5B*^{N642H} induces NK-cell leukemia in mice

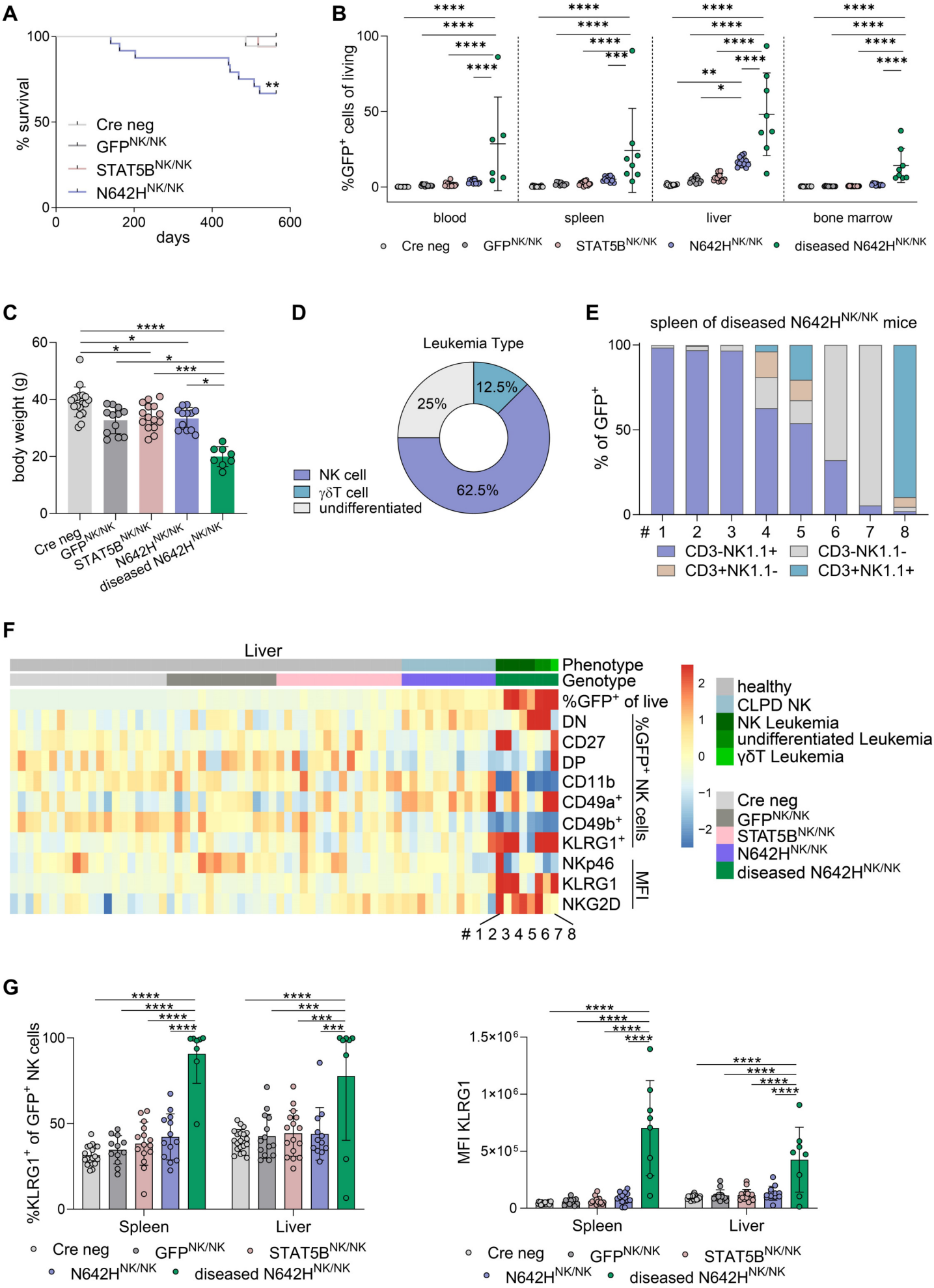

Figure 6: *STAT5B*^{N642H} induces transplantable NK-cell leukemia in mice

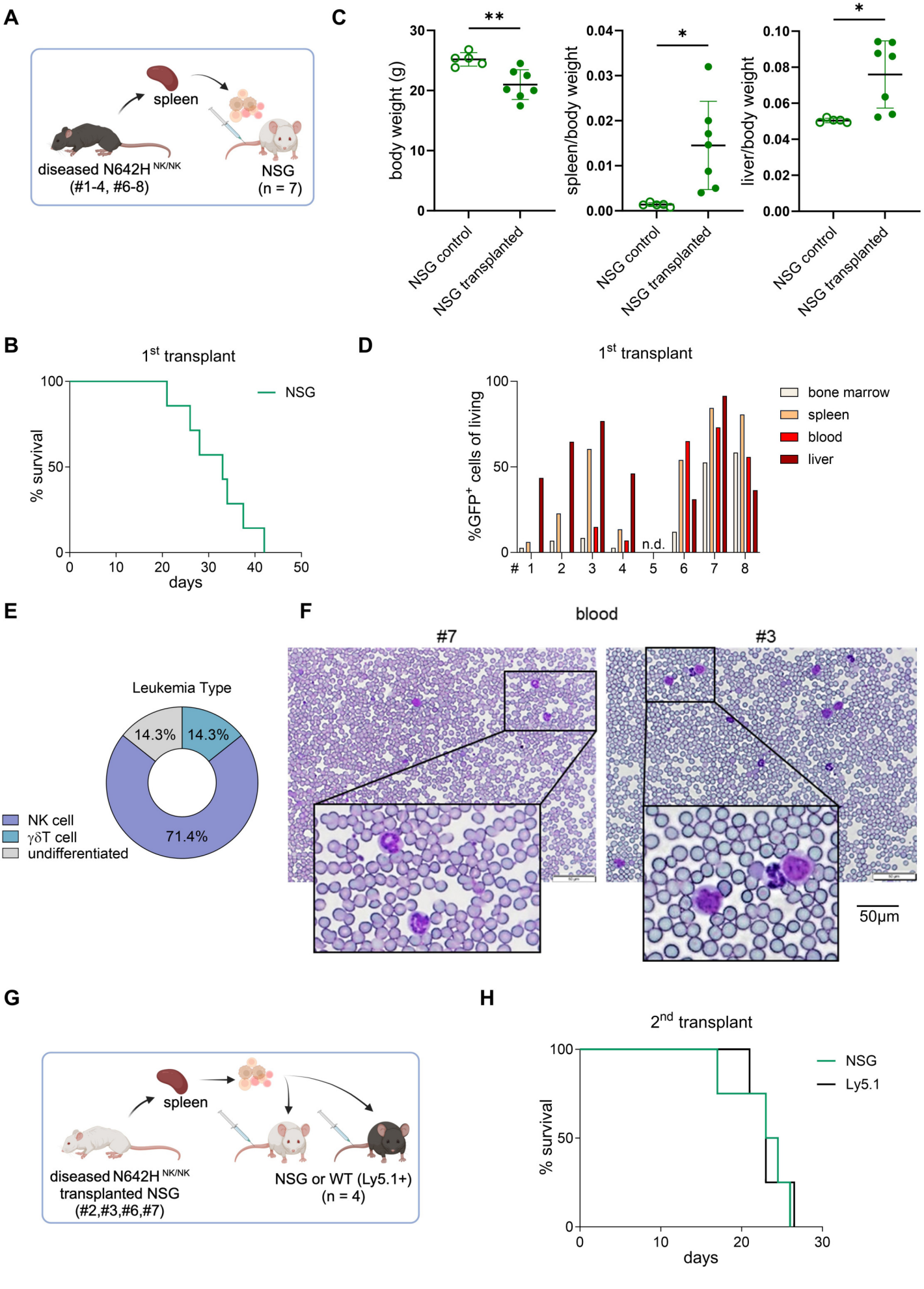

Figure 7: Diseased N642H$^{NK/NK}$ NK cells display molecular features of NK-cell leukemia patients harboring *STAT5B* GOF mutations

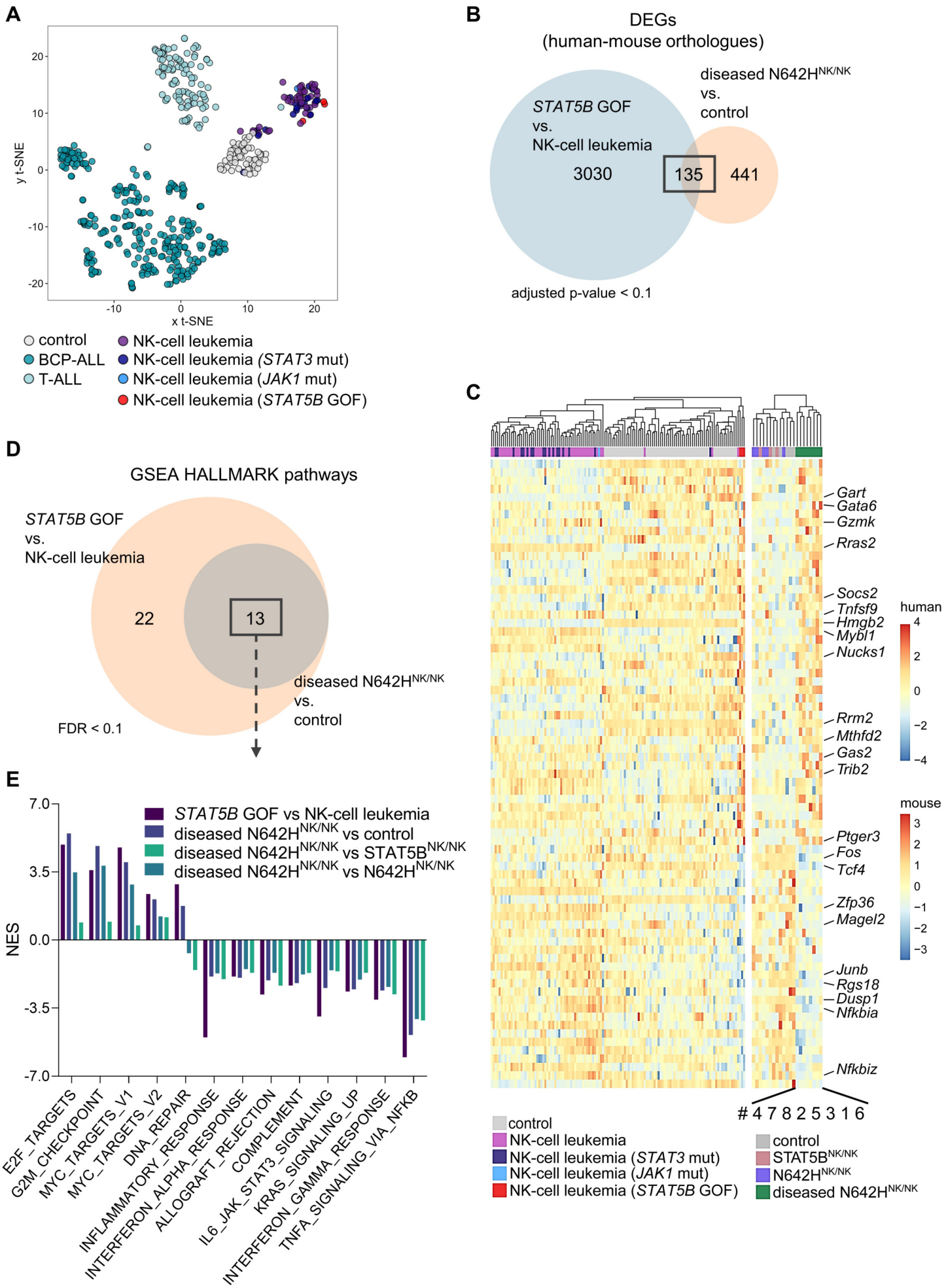

A Lineage-Specific *STAT5B*^{N642H} Mouse Model To Study Natural Killer (NK)-Cell Leukemia

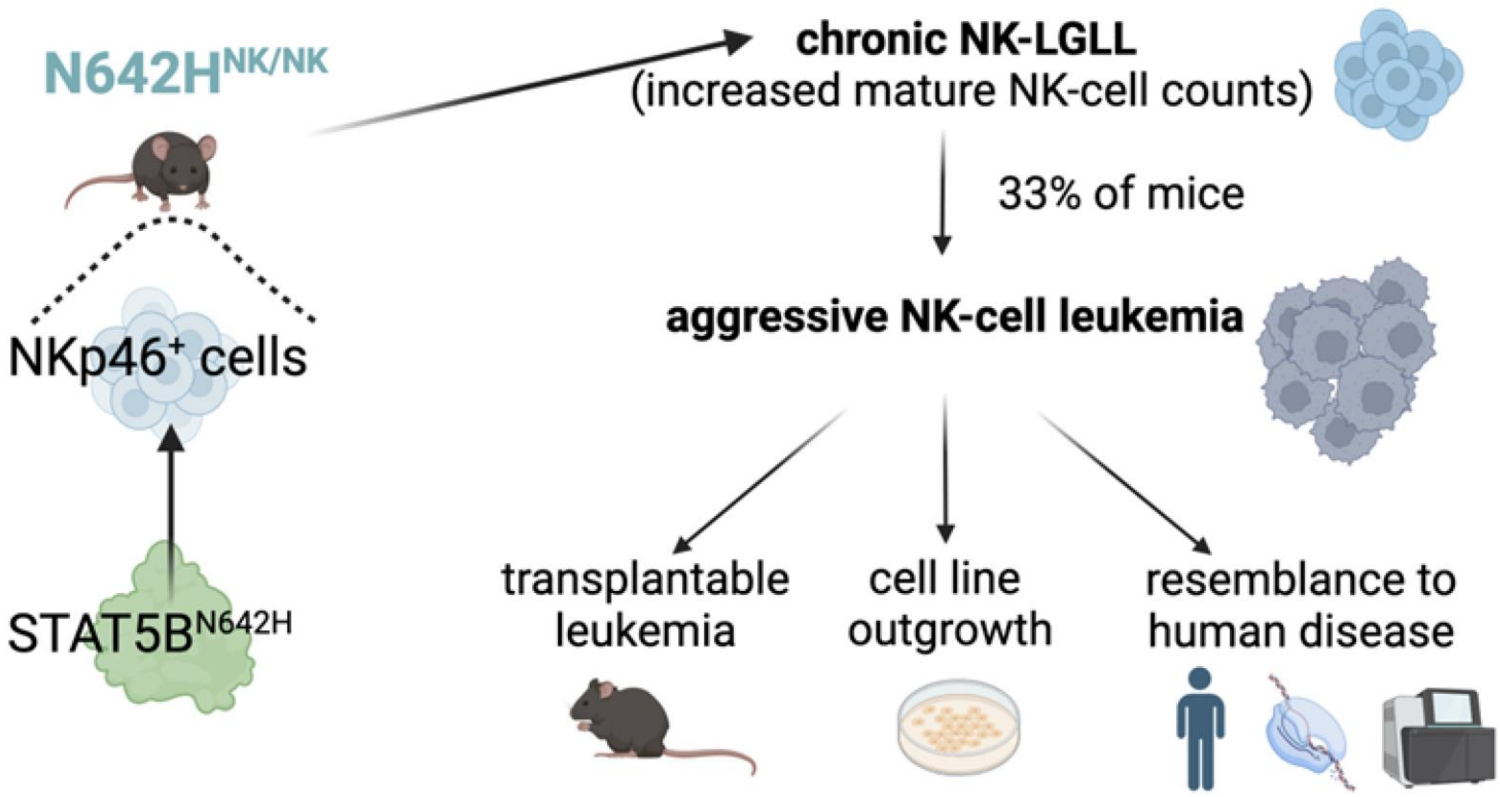

Conclusions: 1) Lineage-specific *STAT5B*^{N642H} transgenic mice (N642H$^{NK/NK}$) develop NK-cell leukemia. 2) *STAT5B*-mutated leukemic NK cells share unique transcriptional profile in mice and human patients.

*Klein et al. DOI: 10.xxxx/**blood**.2023xxxxxx.*

***Blood* Visual Abstract**